AIMS Mathematics, 11(3): 6437–6463.
DOI: 10.3934/math.2026266
Received: 15 January 2026
Revised: 27 February 2026
Accepted: 11 March 2026
Published: 13 March 2026

https://www.aimspress.com/journal/Math

Research article

Complex coexistence induced by delays in a diffusive intraguild predation system with stage structure and spatial memory

Shuai Li[1,2,*], **Bin Fang**[1,2], **Xinyu Song**[1,2] **and Chengdai Huang**[1,2]

[1] College of Mathematics and Statistics, Xinyang Normal University, Xinyang 464000, China

[2] Henan Provincial Center for Applied Mathematics, Xinyang Normal University, Xinyang 464000, China

* **Correspondence:** Email: xynu_sx_lishuai@163.com.

Abstract: We study Hopf bifurcations induced by spatial memory and stage structure in a diffusive intraguild predation system, aiming to reveal their effects on the spatiotemporal dynamics of three interacting species. First, by applying the geometric approach, we obtain the stability criteria and Hopf bifurcation conditions through an analysis of the linearized system with delay-dependent coefficients. Next, we develop a computational algorithm for the normal form of Hopf bifurcation induced by maturation delay in a system with three state variables and diffusion terms containing a delay. Finally, we combine numerical simulations to demonstrate that variations in periods of maturation and spatial memory can generate rich and complex coexistence dynamics, including spatially homogeneous periodic solutions, spatially heterogeneous periodic solutions with mode−5, and multiple stability switches.

Keywords: delays; diffusive predator-prey system; stability; Hopf bifurcation; normal form
Mathematics Subject Classification: 37L10, 92B05, 92D25

1. Introduction

Intraguild predation is a common ecological process where both predation and competition occur simultaneously in the interactions between predators and prey [1, 2]. A feature of intraguild predation is competition between prey and predators arising from the consumption of shared resources [3,4]. The following dynamical model was proposed in the pioneering works [5, 6] of Holt and Polis to capture intraguild predation:

$$\begin{cases} \dfrac{\mathrm{d}R}{\mathrm{d}t} = rR\left(1 - \dfrac{R}{k} - e_1C - e_2P\right), \\ \dfrac{\mathrm{d}C}{\mathrm{d}t} = C\left(\varepsilon_1 e_1 R - \delta_2 - e_3 P\right), \\ \dfrac{\mathrm{d}P}{\mathrm{d}t} = P\left(\varepsilon_2 e_2 R + \varepsilon_3 e_3 C - \delta_3\right). \end{cases} \tag{1.1}$$

In Model (1.1), $R(t)$, $C(t)$, and $P(t)$ represent the population densities of the basal resource, prey, and predators at time t, respectively. The basal resource follows logistic growth with intrinsic growth rate r and carrying capacity k. The predation and conversion rates are defined as follows: e_1 and ε_1 for the prey and e_2, ε_2 and e_3, ε_3 for the predators acting on the shared resource and the prey, respectively. The death rates of the prey and predators are denoted by δ_2 and δ_3. They demonstrate that prey dominance in resource competition and the benefits predators obtain from consuming prey facilitate coexistence. Subsequently, many authors have extended Model (1.1) by incorporating additional biological processes such as the Allee effect [7, 8].

It is worth noting that many ecological processes in nature are not instantaneous. In particular, some species can undergo multiple life stages; during the immature stage, for example, their fecundity can be neglected [9–11]. For instance, the authors of these sources incorporated a delay-dependent parameter in model to describe the maturation period of predators [12, 13]. To capture the stage structure of the intraguild prey, Xu et al. [14] proposed a three-species system with a delay-dependent parameter under the assumption that immature prey neither exploits basal resources nor is subject to predation:

$$\begin{cases} \dfrac{\mathrm{d}R}{\mathrm{d}t} = rR\left(1 - \dfrac{R}{k} - e_1C - e_2P\right), \\ \dfrac{\mathrm{d}C}{\mathrm{d}t} = \varepsilon_1 e_1 R_\tau C_\tau \mathrm{e}^{-\delta_1 \tau} - \delta_2 C - e_3 CP, \\ \dfrac{\mathrm{d}P}{\mathrm{d}t} = P\left(\varepsilon_2 e_2 R + \varepsilon_3 e_3 C - \delta_3\right), \end{cases}$$

where $R_\tau = R(t-\tau)$, $C_\tau = C(t-\tau)$, and τ and δ_1 represent the length and the death rate of the juvenile prey. They demonstrate that maturation delay can induce temporal oscillatory coexistence through a Hopf bifurcation.

Species movement patterns have been recognized as determinants of spatiotemporal distribution [15–17]. Reaction–diffusion equation models are commonly used to describe species dispersal and related biotic processes, especially when field data are limited [18]. For example, Sun et al. [19] incorporated Laplacian and advection terms to describe the random and directed movements of species, showing that random movement can generate diverse patterns through Turing bifurcations, whereas directed movement can lead to traveling patterns. The authors in [20] rigorously derived the modeling procedure for incorporating stage structure, characterized by delay-dependent parameters, into a diffusive predator–prey system. Note that the prey can mitigate predation risk by adopting diverse antipredator strategies [21]. In response to both interspecific competition and predation pressure, the prey can actively disperse away from predators. To incorporate this avoidance mechanism into a mathematical framework, the authors in [22] developed the following model:

$$\begin{cases} \dfrac{\partial R}{\partial t} = \kappa_{11} R_{xx} + rR\left(1 - \frac{R}{k}\right) - e_1 RC - e_2 RP, \quad x \in (0, \iota\pi), \\ \dfrac{\partial C}{\partial t} = \kappa_{22} C_{xx} + \kappa_{23}(CP_x(x,t))_x + \varepsilon_1 e_1 RC - \delta_2 C - e_3 CP, \quad x \in (0, \iota\pi), \\ \dfrac{\partial P}{\partial t} = \kappa_{33} P_{xx} + \varepsilon_2 e_2 RP + \varepsilon_3 e_3 CP - \delta_3 P, \quad x \in (0, \iota\pi), \\ R_x(x,t) = C_x(x,t) = P_x(x,t) = 0, \ x = 0, \ \iota\pi, \end{cases}$$

where κ_{11}, κ_{22}, and κ_{33} denote the random movement rates of the shared resource, prey, and predators, respectively, and κ_{23} represents the prey's avoidance response to predators. They showed that antipredator behavior can give rise to segregation patterns. Notably, numerous species with advanced evolutionary traits can undergo memory-mediated directional movement [23–25]. For example, migration in mule deer is shaped by spatial memory of previously encountered locations, leading to reduced predation risk [26]. Shi et al. [27] pioneered a modeling framework for memory-mediated directional movement by incorporating a time delay into the advection term. Subsequently, the authors in [28] characterized the antipredator behavior of intelligent prey by incorporating a time delay σ into the convection term.

As far as we know, the mechanisms underlying the spatiotemporal distribution of three interacting species in the presence of stage structure and spatial memory have not been thoroughly investigated. Building on the modeling framework of [14, 20, 22, 28], we study an intraguild predation system that incorporates spatial memory and stage structure in the intelligent prey, assuming that the movement of immature prey is limited:

$$\begin{cases} \dfrac{\partial R}{\partial t} = \kappa_{11} R_{xx} + rR\left(1 - \frac{R}{k}\right) - e_1 RC - e_2 RP, \quad x \in (0, \iota\pi), \\ \dfrac{\partial C}{\partial t} = \kappa_{22} C_{xx} + \kappa_{23}(CP_x(x, t-\sigma))_x + \varepsilon_1 e_1 R_\tau C_\tau \mathrm{e}^{-\delta_1 \tau} - \delta_2 C - e_3 CP, \quad x \in (0, \iota\pi), \\ \dfrac{\partial P}{\partial t} = \kappa_{33} P_{xx} + \varepsilon_2 e_2 RP + \varepsilon_3 e_3 CP - \delta_3 P, \quad x \in (0, \iota\pi), \\ R_x(x,t) = C_x(x,t) = P_x(x,t) = 0, \ x = 0, \ \iota\pi, \end{cases} \tag{1.2}$$

where σ represents mean memory duration of the prey. The initial functions $R^0(x,t)$, $C^0(x,t)$, and $P^0(x,t)$ satisfy $R^0(x,t)$, $C^0(x,t)$, $P^0(x,t) \in C^{2+\alpha, 1+\frac{\alpha}{2}}([0, \iota\pi] \times [-\max\{\tau, \sigma\}, 0])$ for some $\alpha \in (0,1)$, together with Neumann boundary conditions $\partial R^0(x,t)/\partial x = \partial C^0(x,t)/\partial x = \partial P^0(x,t)/\partial x = 0$, $t \in [-\max\{\tau, \sigma\}, 0]$, $x = 0$, $x = \iota\pi$. Recently, there has been growing interest in analyzing bifurcations of diffusive systems, as they often signal the formation of new and distinct spatial patterns [29, 30]. For example, the authors in [31, 32] analyzed Hopf and double Hopf bifurcations induced by the spatial memory of two interacting species, showing that it can produce spatially heterogeneous patterns with periodic oscillations on the timescale. However, the Hopf bifurcations generated by memory delay σ and maturation delay τ of System (1.2) with three state variables have not yet been explored. In this paper, we will devote ourselves to studying the mechanisms underlying the spatiotemporal distributions generated by Hopf bifurcations in System (1.2). The principal contributions and novelties of the present study are as follows:

- In contrast to the study in [14,22], we incorporate spatial factor and memory-mediated directional movement of prey into the intraguild predation framework. The resulting System (1.2) applies to scenarios in which prey uses spatial memory to avoid areas frequented by predators, thereby reducing predation risk under the combined pressures of competition and predation.
- We employ the stability switching curves method from [33] to identify stable regions in the (τ, σ)-plane without preassigning either delay. Additionally, we numerically determine the critical values of the maturation delay τ for given memory delay σ.
- We extend the calculation algorithm of normal form for Hopf bifurcations from [31] to System (1.2), accommodating multiple species and the delay in the reaction term. Notably, our method can also address mode-0 Hopf bifurcation, extending the scope beyond that of [34].

We establish a framework to elucidate how spatial memory and stage structure drive the spatiotemporal patterns of more than two interacting species through Hopf bifurcation.

The remainder of this paper is organized as follows. In Section 2, we analyze the linearized system (1.2) via the stability switching curves approach to identify Hopf bifurcation values. Section 3 is devoted to deriving the third-order normal form associated with the Hopf bifurcation generated by the maturation delay τ. Numerical experiments validating the theoretical analysis are presented in Section 4. Finally, concluding remarks are given in Section 5.

2. Linear stability and Hopf bifurcation of System (1.2)

In this section, we first discuss the well-posedness of System (1.2). Then, we determine the linear stability regions in the (τ, σ)-plane using the stability switching curves method and thereby obtain the critical values of τ and σ corresponding to Hopf bifurcations. The result guarantees the unique existence of a positive solution for System (1.2).

Lemma 1. *Assume the initial functions $C^0(x,t), R^0(x,t), P^0(x,t) \geq 0$ with $C^0(x,t), R^0(x,t), P^0(x,t) \not\equiv 0$. Then, System (1.2) admits a unique positive solution $(C(x,t), R(x,t), P(x,t))$ defined for all $t \geq 0$. Moreover, the solution satisfies*

$$\limsup_{t\to\infty} R(x,t) \leq k,\ \limsup_{t\to\infty} \int_0^{\iota\pi} C(x,t)\mathrm{d}x \leq M_1,\ \limsup_{t\to\infty} \int_0^{\iota\pi} P(x,t)\mathrm{d}x \leq M_2,$$

with

$$M_1 = \frac{\varepsilon_1 \mathrm{e}^{-\delta_1\tau}\iota\pi k\,(r+\delta_2)}{\delta_2}, \quad M_2 = \frac{k\iota\pi\left(\varepsilon_2 r + \varepsilon_1\varepsilon_3 e_1 \mathrm{e}^{-\delta_1\tau} M_1 + \delta\varepsilon_2\right)}{\delta}$$

and $\delta = \min\{\delta_2, \delta_3\}$.

Proof. Without loss of generality, we assume $\tau > \sigma$. It follows from [35, Theorem 1] that System (1.2) admits a unique positive solution for any $[k\sigma, (k+1)\sigma]$ with $k \geq 0$. We can observe that $R(x,t)$ meets

$$\begin{cases} \dfrac{\partial R}{\partial t} \leq \kappa_{11} R_{xx} + rR\left(1 - \frac{R}{k}\right), & x \in (0, \iota\pi), \\ R_x(x,t) = 0,\ x = 0,\ \iota\pi. \end{cases}$$

Applying the comparison principle, it follows that

$$\limsup_{t\to\infty} R(x,t) \leq k.$$

Therefore, for any ξ, there exists a $T_1 > 0$ such that

$$R(x,t) \le (k+\xi), \text{ for } t \ge T_1.$$

Denote

$$\mathcal{U}_1(t) = \int_0^{\iota\pi} R(x,t)\mathrm{d}x,\ \mathcal{U}_2(t) = \int_0^{\iota\pi} C(x,t)\mathrm{d}x,\ \mathcal{U}_3(t) = \int_0^{\iota\pi} P(x,t)\mathrm{d}x.$$

We can deduce from the Neumman boundary conditions that

$$\begin{aligned}\frac{\mathrm{d}\left(\varepsilon_1 \mathrm{e}^{-\delta_1\tau}\mathcal{U}_1(t) + \mathcal{U}_2(t+\tau)\right)}{\mathrm{d}t} &\le \varepsilon_1 r\mathrm{e}^{-\delta_1\tau}\mathcal{U}_1(t) - \delta_2\mathcal{U}_2(t+\tau)\\ &\le \varepsilon_1\mathrm{e}^{-\delta_1\tau}\iota\pi(k+\xi)(r+\delta_2) - \delta_2\left(\varepsilon_1\mathrm{e}^{-\delta_1\tau}\mathcal{U}_1(t) + \mathcal{U}_2(t+\tau)\right),\ t > T_1.\end{aligned}$$

It follows from the comparison principle that

$$\limsup_{t\to\infty}\left(\varepsilon_1\mathrm{e}^{-\delta_1\tau}\mathcal{U}_1(t) + \mathcal{U}_2(t+\tau)\right) \le \frac{\varepsilon_1\mathrm{e}^{-\delta_1\tau}\iota\pi k(r+\delta_2)}{\delta_2} := M_1.$$

Similarly, there exists a $T_2 > T_1$ such that $\mathcal{U}_2(t) = \int_0^{\iota\pi} C(x,t)\mathrm{d}x \le M_1 + \xi$ for $t > T_2$. We can thus deduce that

$$\begin{aligned}&\frac{\mathrm{d}\left(\varepsilon_2\mathcal{U}_1(t) + \varepsilon_3\mathcal{U}_2(t) + \mathcal{U}_3(t)\right)}{\mathrm{d}t}\\ \le&\varepsilon_2 r\mathcal{U}_1(t) + \varepsilon_1\varepsilon_3 e_1\mathrm{e}^{-\delta_1\tau}(k+\xi)(M_1+\xi)\iota\pi - \varepsilon_3\delta_2\mathcal{U}_2(t) - \delta_3\mathcal{U}_3(t)\\ \le&(k+\xi)\iota\pi\left(\varepsilon_2 r + \varepsilon_1\varepsilon_3 e_1\mathrm{e}^{-\delta_1\tau}(M_1+\xi) + \delta\varepsilon_2\right) - \delta(\varepsilon_2\mathcal{U}_1(t) + \varepsilon_3\mathcal{U}_2(t) + \mathcal{U}_3(t)),\ t \ge T_2+\tau\end{aligned}$$

with $\delta = \min\{\delta_2, \delta_3\}$. It then follows that

$$\limsup_{t\to\infty}\left(\varepsilon_2\mathcal{U}_1(t) + \varepsilon_3\mathcal{U}_2(t) + \mathcal{U}_3(t)\right) \le \frac{k\iota\pi\left(\varepsilon_2 r + \varepsilon_1\varepsilon_3 e_1\mathrm{e}^{-\delta_1\tau}M_1 + \delta\varepsilon_2\right)}{\delta} := M_2.$$

Accordingly, we obtain

$$\limsup_{t\to\infty}\int_0^{\iota\pi} P(x,t)\mathrm{d}x \le M_2.$$

□

Denote

$$\begin{aligned}D(\tau) &= \frac{e_3}{k}\left(\varepsilon_1\varepsilon_3 e_1 e_2 k e^{-\delta_1\tau} + r\varepsilon_3 e_3 - k e_1 e_2\varepsilon_2\right),\\ D_1 &= e_3\left(\delta_2 e_2\varepsilon_3 + r\varepsilon_3 e_3 - \delta_3 e_1\right),\\ D_2(\tau) &= \frac{1}{k}\left(\varepsilon_1 e_1 e_2\delta_3 k e^{-\delta_1\tau} - rke_2 e_3\varepsilon_2 - k\delta_2 e_2^2\varepsilon_2 + re_3\delta_3\right),\\ D_3(\tau) &= \frac{1}{k}\left(\varepsilon_2 e_1 e_2\delta_2 k + \varepsilon_1\varepsilon_3 e_1 e_3 kre^{-\delta_1\tau} - \varepsilon_1 e_1^2 k\delta_3 e^{-\delta_1\tau} - r\varepsilon_3 e_3\delta_2\right).\end{aligned}$$

Because our study is ecologically motivated by the coexistence of species, we narrow our focus to the coexistence equilibrium and introduce the following assumptions to ensure the existence of a constant steady state:

$$(\mathbf{H}1) \qquad \frac{D_1}{D(\tau)} > 0,\ \frac{D_2(\tau)}{D(\tau)} > 0,\ \frac{D_3(\tau)}{D(\tau)} > 0.$$

Accordingly, System (1.2) has a unique constant steady state

$$E^*(\tau) = (R^*(\tau), C^*(\tau), P^*(\tau)) = \left(\frac{D_1}{D(\tau)}, \frac{D_2(\tau)}{D(\tau)}, \frac{D_3(\tau)}{D(\tau)}\right).$$

The linearized system of System (1.2) at $E^*(\tau)$ is given by

$$\begin{cases} \dfrac{\partial R}{\partial t} = \kappa_{11} R_{xx} + a_{11}(\tau) R(x,t) + a_{12}(\tau) C(x,t) + a_{13}(\tau) P(x,t), \\ \dfrac{\partial C}{\partial t} = \kappa_{22} C_{xx} + \kappa_{23} C^*(\tau) P_{xx}(x, t-\sigma) + a_{22}(\tau) C(x,t) + a_{23}(\tau) P(x,t), \\ \qquad + b_{21}(\tau) R(x, t-\tau) + b_{22}(\tau) C(x, t-\tau), \\ \dfrac{\partial P}{\partial t} = \kappa_{33} P_{xx} + a_{31}(\tau) R(x,t) + a_{32}(\tau) C(x,t), \\ R_x(x,t) = C_x(x,t) = P_x(x,t) = 0,\ x = 0,\ \iota\pi, \end{cases} \tag{2.1}$$

where

$$\begin{aligned} &a_{11}(\tau) = -\tfrac{rR^*(\tau)}{k}, && a_{12}(\tau) = -e_1 R^*(\tau), && a_{13}(\tau) = -e_2 R^*(\tau), \\ &a_{22}(\tau) = -(\delta_2 + e_3 P^*(\tau)), && a_{23}(\tau) = -e_3 C^*(\tau), && a_{31}(\tau) = \varepsilon_2 e_2 P^*(\tau), \\ &a_{32}(\tau) = \varepsilon_3 e_3 P^*(\tau), && b_{21}(\tau) = \varepsilon_1 e_1 C^*(\tau) \mathrm{e}^{-\delta_1 \tau}, && b_{22}(\tau) = \varepsilon_1 e_1 R^*(\tau) \mathrm{e}^{-\delta_1 \tau}. \end{aligned} \tag{2.2}$$

This leads to the following characteristic equation for System (2.1):

$$J(\lambda; n, \tau, \sigma) = f_0(\lambda; n, \tau) + f_1(\lambda; n, \tau)\mathrm{e}^{-\lambda\tau} + f_2(\lambda; n, \tau)\mathrm{e}^{-\lambda\sigma} = 0, \tag{2.3}$$

where

$$\begin{aligned} f_0(\lambda; n, \tau) &= \lambda^3 + f_{02}(n,\tau)\lambda^2 + f_{01}(n,\tau)\lambda + f_{00}(n,\tau), \\ f_1(\lambda; n, \tau) &= f_{12}(\tau)\lambda^2 + f_{11}(n,\tau)\lambda + f_{10}(n,\tau), \\ f_2(\lambda; n, \tau) &= f_{21}(n,\tau)\lambda + f_{20}(n,\tau), \end{aligned}$$

with

$$\begin{aligned} f_{02}(n,\tau) =& (\kappa_{11} + \kappa_{22} + \kappa_{33})\left(\frac{n}{\iota}\right)^2 - a_{11}(\tau) - a_{22}(\tau), \\ f_{01}(n,\tau) =& ((\kappa_{11} + \kappa_{22})\kappa_{33} + \kappa_{11}\kappa_{22})\left(\frac{n}{\iota}\right)^4 + a_{11}(\tau)a_{22}(\tau) - a_{13}(\tau)a_{31}(\tau) - a_{23}(\tau)a_{32}(\tau) \\ &- ((a_{11}(\tau) + a_{22}(\tau))\kappa_{33} + \kappa_{11}a_{22}(\tau) + \kappa_{22}a_{11}(\tau))\left(\frac{n}{\iota}\right)^2, \\ f_{00}(n,\tau) =& \kappa_{11}\kappa_{22}\kappa_{33}\left(\frac{n}{\iota}\right)^6 - (a_{11}(\tau)\kappa_{22} + a_{22}(\tau)\kappa_{11})\kappa_{33}\left(\frac{n}{\iota}\right)^4 + a_{11}(\tau)a_{23}(\tau)a_{32}(\tau) \\ &+ (a_{11}(\tau)a_{22}(\tau)\kappa_{33} - a_{13}(\tau)a_{31}(\tau)\kappa_{22} - a_{23}(\tau)a_{32}(\tau)\kappa_{11})\left(\frac{n}{\iota}\right)^2 \end{aligned}$$

$$
\begin{aligned}
&+ a_{31}(\tau)(a_{13}(\tau)a_{22}(\tau) - a_{12}(\tau)a_{23}(\tau)),\\
f_{12}(\tau) =& - b_{22}(\tau),\\
f_{11}(n,\tau) =& b_{22}(\tau)\left(a_{11}(\tau) - (\kappa_{11}+\kappa_{33})\left(\frac{n}{\iota}\right)^2\right) - a_{12}(\tau)b_{21}(\tau),\\
f_{10}(n,\tau) =& b_{22}(\tau)\left(a_{13}(\tau)a_{31}(\tau) - \kappa_{33}\left(\kappa_{11}\left(\frac{n}{\iota}\right)^4 - a_{11}(\tau)\left(\frac{n}{\iota}\right)^2\right)\right)\\
&- b_{21}(\tau)\left(\left(\frac{n}{l}\right)^2 a_{12}(\tau)\kappa_{33} + a_{13}(\tau)a_{32}(\tau)\right),\\
f_{21}(n,\tau) =& \kappa_{23}a_{32}(\tau)C^*(\tau)\left(\frac{n}{\iota}\right)^2,\\
f_{20}(n,\tau) =& \kappa_{23}C^*(\tau)\left(\frac{n}{\iota}\right)^2\left(\left(\kappa_{11}\left(\frac{n}{\iota}\right)^2 - a_{11}(\tau)\right)a_{32}(\tau) + a_{12}(\tau)a_{31}(\tau)\right).
\end{aligned}
$$

The characteristic equation (2.3) coincides with that in [14] when $k = 0$, which allows us to directly adopt their results to determine the stability intervals of τ. Subsequently, we apply the technique developed in [33] to analyze (2.3), which allows us to delineate the stable regions in the (τ, σ)-plane and to determine the critical values associated with Hopf bifurcation. We substitute $\lambda = i\chi$ into Eq (2.3) and rewrite it as follows:

$$1 + \beta_1(\chi; n, \tau)\mathrm{e}^{-i\chi\tau} + \beta_2(\chi; n, \tau)\mathrm{e}^{-i\chi\sigma} = 0, \tag{2.4}$$

where

$$\beta_1(\chi; n, \tau) = \frac{f_1(i\chi; n, \tau)}{f_0(i\chi; n, \tau)},\ \beta_2(\chi; n, \tau) = \frac{f_2(i\chi; n, \tau)}{f_0(i\chi; n, \tau)}.$$

Equation (2.4) indicates that $1, \beta_1(\chi; n, \tau)\mathrm{e}^{-i\chi\tau}$, and $\beta_2(\chi; n, \tau)\mathrm{e}^{-i\chi\sigma}$ can form a triangle in the complex plane. Consequently, for a fixed wavenumber n, the feasible regions Ω^n of (χ, τ) can be determined by the following inequalities:

$$
\begin{aligned}
&|\beta_1(\chi; n, \tau)| + |\beta_2(\chi; n, \tau)| \geq 1,\\
&|\beta_1(\chi; n, \tau)| - |\beta_2(\chi; n, \tau)| \leq 1,\\
&|\beta_2(\chi; n, \tau)| - |\beta_1(\chi; n, \tau)| \leq 1.
\end{aligned} \tag{2.5}
$$

Let $\theta_1(\chi; n, \tau)$ and $\theta_2(\chi; n, \tau)$ be the interior angles of the triangle opposited by sides $\beta_2(\chi; n, \tau)\mathrm{e}^{-i\chi\sigma}$ and $\beta_1(\chi; n, \tau)\mathrm{e}^{-i\chi\tau}$, respectively. We can deduce from the the law of cosines that

$$
\begin{aligned}
\theta_1(\chi; n, \tau) &= \arccos\left(\frac{1 + |\beta_1(\chi; n, \tau)|^2 - |\beta_2(\chi; n, \tau)|^2}{2|\beta_1(\chi; n, \tau)|}\right),\\
\theta_2(\chi; n, \tau) &= \arccos\left(\frac{1 + |\beta_2(\chi; n, \tau)|^2 - |\beta_1(\chi; n, \tau)|^2}{2|\beta_2(\chi; n, \tau)|}\right).
\end{aligned}
$$

We further define

$$\mathcal{S}_m^{\pm}(\chi; n, \tau) = \chi\tau - (\arg(\beta_1(\chi; n, \tau)) \pm \theta_1(\chi; n, \tau) + (2m-1)\pi),\ \text{for } m \in \mathbb{N}. \tag{2.6}$$

For a fixed χ in the feasible region, if there exist $\tau_m^{\pm}$ satisfying $\mathcal{S}_m^{\pm}(\chi; n, \tau_m^{\pm}) = 0$, we substitute them into the following equation to derive the corresponding expression for σ:

$$\sigma_l^{\pm} = \frac{1}{\chi}(\arg(\beta_2(\chi; n, \tau_m^{\pm})) \mp \theta_2(\chi; n, \tau_m^{\pm}) + (2l-1)\pi),\ \text{for } l \in \mathbb{N}. \tag{2.7}$$

Therefore, we can derive the following crossing curves along which Eq (2.3) admits purely imaginary roots:

$$C^n = \{(\tau_m^{\pm}(n), \sigma_l^{\pm}(n)), \text{ for } m,\ l \in \mathbb{N}\}.$$

We also need to determine the crossing direction in order to identify whether Eq (2.3) admits two additional positive real roots to the left or to the right of the crossing curves C^n [33]. For fixed n, we define

$$\begin{aligned}
\mathcal{M}_1(\tau,\sigma) &= \Re\left(\frac{\partial J(\lambda;n,\tau,\sigma)}{\partial\tau}\right),\\
\mathcal{N}_1(\tau,\sigma) &= \Im\left(\frac{\partial J(\lambda;n,\tau,\sigma)}{\partial\tau}\right),\\
\mathcal{M}_2(\tau,\sigma) &= \Re\left(\frac{\partial J(\lambda;n,\tau,\sigma)}{\partial\sigma}\right),\\
\mathcal{N}_2(\tau,\sigma) &= \Im\left(\frac{\partial J(\lambda;n,\tau,\sigma)}{\partial\sigma}\right).
\end{aligned}$$

Therefore, we can apply the following results to judge the stable and unstable regions on the (τ,σ)-plane.

Theorem 1. *Equation* (2.3) *possesses a pair of purely imaginary roots* $\pm i\chi_n$ *when* $(\tau,\sigma) = (\tau_n^H, \sigma_n^H)$ *lies on the crossing curves* C^n. *Furthermore, as* (τ,σ) *crosses* (τ_n^H, σ_n^H) *and enters the region to the right (left) of* C^n, *two eigenvalues of Eq* (2.3) *acquire positive real parts if*

$$\mathcal{M}_1(\tau_n^H,\sigma_n^H)\mathcal{N}_2(\tau_n^H,\sigma_n^H) - \mathcal{M}_2(\tau_n^H,\sigma_n^H)\mathcal{N}_1(\tau_n^H,\sigma_n^H) > 0 (< 0).$$

Remark 1. *By employing the stability switching curves method introduced in [33], the derivation of Hopf bifurcation conditions is greatly simplified, and stable regions in the* (τ,σ)*-plane can be identified without preassigning either delay [36]. Furthermore, it suffices to plot the crossing curves for finite wave numbers n because the first inequality in* (2.5) *fails to hold for sufficiently large n.*

Remark 2. *When* (τ_n^H, σ_n^H) *lies on the boundary of the stable region, it is classified as a Hopf bifurcation point. For a fixed value of* σ, *the critical Hopf bifurcation values can be obtained by computing the intersection of curves* (2.6) *and* (2.7) *in the* (χ,τ)*-plane using Matlab.*

3. Hopf bifurcation with respect to the delay parameter τ: normal form

This section is devoted to deriving the normal form induced by the maturation delay τ, which allows us to determine the Hopf bifurcation direction and the stability of the emerging periodic orbits. For simplicity in notation, we write the Hopf bifurcation point (τ_n^H, σ_n^H) and the corresponding critical values n and χ_n as (τ^H, σ^H), n_H and χ_{n_H}, respectively. Assume, without loss of generality, that $\tau^H < \sigma^H$.

We first perform the following time-scale transformation to normalize τ:

$$U(x,t) = \begin{pmatrix} U^{(1)}(x,t) \\ U^{(2)}(x,t) \\ U^{(3)}(x,t) \end{pmatrix} = \begin{pmatrix} R(x,t\tau) \\ C(x,t\tau) \\ P(x,t\tau) \end{pmatrix}.$$

Consequently, System (1.2) becomes

$$\begin{cases} \dfrac{\partial U^{(1)}}{\partial t} = \kappa_{11}\tau U^{(1)}_{xx} + r\tau U^{(1)}\left(1 - \dfrac{U^{(1)}}{k}\right) - \tau e_1 U^{(1)}U^{(2)} - \tau e_2 U^{(1)}U^{(3)}, \ x \in (0, \iota\pi), \\ \dfrac{\partial U^{(2)}}{\partial t} = \kappa_{22}\tau U^{(1)}_{xx} + \kappa_{23}\tau\left(U^{(2)}U^{(3)}_x\left(x, t - \dfrac{\sigma}{\tau}\right)\right)_x + \tau\varepsilon_1 e_1 \mathrm{e}^{-\delta_1\tau}U^{(1)}(x, t-1)U^{(2)}(x, t-1), \\ \qquad\qquad - \tau\delta_2 U^{(2)} - \tau e_3 U^{(2)}U^{(3)}, \ x \in (0, \iota\pi), \\ \dfrac{\partial U^{(3)}}{\partial t} = \tau\kappa_{33}U^{(3)}_{xx} + \tau\varepsilon_2 e_2 U^{(1)}U^{(3)} + \tau\varepsilon_3 e_3 U^{(2)}U^{(3)} - \tau\delta_3 U^{(3)}, \quad x \in (0, \iota\pi), \\ U^{(1)}_x(x,t) = U^{(2)}_x(x,t) = U^{(3)}_x(x,t), \ x = 0, \ x = \iota\pi, \end{cases} \tag{3.1}$$

with phase space

$$C_1 := C\left(\left[-\frac{\sigma}{\tau}, 0\right], \mathcal{H}\right),$$

where

$$\mathcal{H} = \{U = (U^{(1)}, U^{(2)}, U^{(3)})^{\mathrm{T}} \in (W^{2,2}(0, \iota\pi))^3 : U^{(i)}_x(0) = U^{(i)}_x(\iota\pi) = 0, i = 1, 2, 3\},$$

endowed with the inner product

$$[\mathrm{U}, \mathrm{V}] = \int_0^{\iota\pi} \mathrm{U}^{\mathrm{T}}\mathrm{V}\mathrm{d}x, \ \mathrm{U}, \mathrm{V} \in \mathcal{H}.$$

It is customary to define $U_t \in C_1$ by

$$U_t(x, s) = U(x, t + s), \quad (x, s) \in (0, \iota\pi) \times \Big[-\frac{\sigma}{\tau}, 0\Big].$$

We then introduce a small perturbation ε to τ^H by setting

$$\tau = \tau^H + \epsilon,$$

where ϵ will be treated as a state variable in the subsequent analysis. We further denote $V(x, t)$ and σ^H/τ^H by $V(t)$ and σ^0 and let

$$\kappa_0 = \begin{pmatrix} \kappa_{11} & 0 & 0 \\ 0 & \kappa_{22} & 0 \\ 0 & 0 & \kappa_{33} \end{pmatrix},$$

$$\kappa(\tau) = \begin{pmatrix} 0 & 0 & 0 \\ 0 & 0 & \kappa_{23}C^*(\tau) \\ 0 & 0 & 0 \end{pmatrix},$$

$$A(\tau) = \begin{pmatrix} a_{11}(\tau) & a_{12}(\tau) & a_{13}(\tau) \\ 0 & a_{22}(\tau) & a_{23}(\tau) \\ a_{31}(\tau) & a_{32}(\tau) & 0 \end{pmatrix},$$

$$B(\tau) = \begin{pmatrix} 0 & 0 & 0 \\ b_{21}(\tau) & b_{22}(\tau) & 0 \\ 0 & 0 & 0 \end{pmatrix},$$

where $a_{11}(\tau)$, $a_{12}(\tau)$, $a_{13}(\tau)$, $a_{22}(\tau)$ $a_{23}(\tau)$, $a_{31}(\tau)$, $a_{32}(\tau)$, $b_{21}(\tau)$, and $b_{22}(\tau)$ are presented in (2.2).

We perform the following variable transformation to shift the steady state $E^*(\tau)$ of (3.1) to the origin:

$$V(x,t) = \begin{pmatrix} V^{(1)}(x,t) \\ V^{(2)}(x,t) \\ V^{(3)}(x,t) \end{pmatrix} = \begin{pmatrix} V^{(1)}(x,t) - R^*(\tau) \\ V^{(2)}(x,t) - C^*(\tau) \\ V^{(3)}(x,t) - P^*(\tau) \end{pmatrix}.$$

As a consequence, System (3.1) is transformed into

$$\frac{\mathrm{d}V(t)}{\mathrm{d}t} = D(\epsilon)(V_t)_{xx} + L(\epsilon)(V_t) + G(V_t, \epsilon), \tag{3.2}$$

where, for $\rho \in C_1$,

$$\begin{aligned}
D(\epsilon)(\rho)_{xx} =& D(0)(\rho)_{xx} + G^{\kappa}(\rho, \epsilon), \\
L(\epsilon)(\rho) =& (\tau^H + \epsilon)A(\tau^H + \epsilon)\rho(0) + (\tau^H + \epsilon)B(\tau^H + \epsilon)\rho(-1), \\
G(\rho, \epsilon) =& (\tau^H + \epsilon)\begin{pmatrix} g_1(\rho^{(1)}(0) + R^*(\tau), \rho^{(2)}(0) + C^*(\tau), \rho^{(3)}(0) + P^*(\tau)) \\ g_2(\rho^{(1)}(-1) + R^*(\tau), \rho^{(2)}(-1) + C^*(\tau), \rho^{(2)}(0) + C^*(\tau), \rho^{(3)}(0) + P^*(\tau)) \\ g_3(\rho^{(1)}(0) + R^*(\tau), \rho^{(2)}(0) + C^*(\tau), \rho^{(3)}(0) + P^*(\tau)) \end{pmatrix} \\
& - L(\epsilon)(\rho)
\end{aligned}$$

with

$$g_1(\rho^{(1)}(0), \rho^{(2)}(0), \rho^{(3)}(0)) = r\rho^{(1)}(0)\left(1 - \frac{\rho^{(1)}(0)}{k}\right) - e_1\rho^{(1)}(0)\rho^{(2)}(0) - e_2\rho^{(1)}(0)\rho^{(3)}(0)$$

$$\begin{aligned}
g_2(\rho^{(1)}(-1), \rho^{(2)}(-1), \rho^{(2)}(0), \rho^{(3)}(0)) =& \epsilon_1 e_1 \mathrm{e}^{-\delta_1\tau}\rho^{(1)}(-1)\rho^{(2)}(-1) - \delta_2\rho^{(2)}(0) - e_3\rho^{(2)}(0)\rho^{(3)}(0), \\
g_3(\rho^{(1)}(0), \rho^{(2)}(0), \rho^{(3)}(0)) =& \epsilon_2 e_2\rho^{(1)}(0)\rho^{(3)}(0) + \epsilon_3 e_3\rho^{(2)}(0)\rho^{(3)}(0) - \delta_3\rho^{(3)}(0).
\end{aligned}$$

We do some calculations to have

$$D(0)(\rho)_{xx} = \tau^H\kappa_0\rho_{xx}(0) + \tau^H\kappa(\tau^H)\rho_{xx}(-\sigma^0)$$

and

$$\begin{aligned}
G^{\kappa}(\rho, \epsilon) =& \kappa_{23}\epsilon\begin{pmatrix} 0 \\ C^*(\tau^H)\rho^{(3)}_{xx}(-\sigma^0) + \tau^H C^*(\tau^H)\rho^{(3)}_{xx\epsilon}(-\sigma^0) + \tau^H C^*_{\epsilon}(\tau^H)\rho^{(3)}_{xx}(-\sigma^0) \\ 0 \end{pmatrix} \\
& + \epsilon\begin{pmatrix} \kappa_{11}\rho^{(1)}_{xx}(0) \\ \kappa_{22}\rho^{(2)}_{xx}(0) \\ \kappa_{33}\rho^{(3)}_{xx}(0) \end{pmatrix} + \kappa_{23}\tau^H\begin{pmatrix} 0 \\ \rho^{(2)}(0)\rho^{(3)}_{xx}(-\sigma^0) + \rho^{(2)}_x(0)\rho^{(3)}_x(-\sigma^0) \\ 0 \end{pmatrix} + \cdots .
\end{aligned} \tag{3.3}$$

We write System (3.2) as the sum of its linear and nonlinear terms:

$$\frac{\mathrm{d}V(t)}{\mathrm{d}t} = D(0)(V_t)_{xx} + L(0)(V_t) + \widetilde{G}(V_t, \epsilon), \tag{3.4}$$

where $\widetilde{G}(V_t, \epsilon) = G^{\kappa}(V_t, , \epsilon) + (L(\epsilon)(V_t) - L(0)(V_t)) + G(V_t, \epsilon)$. The characteristic equation of

$$\frac{\mathrm{d}V(t)}{\mathrm{d}t} = D(0)(V_t)_{xx} + L(0)(V_t) \tag{3.5}$$

is the same as that of System (2.1).

Denote

$$\beta_n(x) = \frac{\cos\left(\frac{nx}{\iota}\right)}{\|\cos\left(\frac{nx}{\iota}\right)\|_{2,2}} = \begin{cases} \frac{1}{\sqrt{\iota\pi}}, & n = 0, \\ \frac{\sqrt{2}}{\sqrt{\iota\pi}}\cos\left(\frac{nx}{\iota}\right), & n \neq 0, \end{cases}$$

as the eigenfunctions with respect to the eigenvalues $(n/\iota)^2$ of the following system:

$$N''(x) = -sN(x), \quad x \in (0, \iota\pi), \quad N'(0) = N'(\iota\pi) = 0.$$

We define

$$\gamma_n^{(1)}(x) = \beta_n(x)\begin{pmatrix}1\\0\\0\end{pmatrix}, \quad \gamma_n^{(2)}(x) = \beta_n(x)\begin{pmatrix}0\\1\\0\end{pmatrix}, \quad \gamma_n^{(3)}(x) = \beta_n(x)\begin{pmatrix}0\\0\\1\end{pmatrix}$$

and adopt the following space:

$$\Upsilon_n = \left\{[V(\cdot), \gamma_n^{(i)}(x)]\,\gamma_n^{(i)}(x) \;\middle|\; V(\cdot) \in C_1,\ i = 1, 2, 3\right\}.$$

Suppose that $Z_t(\varpi) \in \mathcal{S} := C([-\sigma^0, 0], \mathbb{R}^3)$. Then, on Υ_n, System (3.5) can be reduced to the following system in $\mathcal{S}$:

$$\dot{Z}(t) = L_0^{\kappa}(Z_t(\varpi)) + L(0)(Z_t(\varpi)), \tag{3.6}$$

where

$$L_0^{\kappa}(Z_t(\varpi)) = \tau^H \begin{pmatrix} -\kappa_{11}\left(\frac{n}{\iota}\right)^2 & 0 & 0 \\ 0 & -\kappa_{22}\left(\frac{n}{\iota}\right)^2 & 0 \\ 0 & 0 & -\kappa_{33}\left(\frac{n}{\iota}\right)^2 \end{pmatrix} Z_t(0) + \tau^H \begin{pmatrix} 0 & 0 & 0 \\ 0 & 0 & -\kappa_{23}C^*(\tau^H)\left(\frac{n}{\iota}\right)^2 \\ 0 & 0 & 0 \end{pmatrix} z_t(-\sigma^0).$$

Let $\eta_n(\varpi) \in BV([-\sigma^0, 0], \mathbb{R}^3)$ satisfy

$$\int_{-\sigma^0}^{0} \mathrm{d}\eta_n(\varpi)\,\phi(\varpi) = L_0^{\kappa}(\phi(\varpi)) + L(0)(\phi(\varpi)), \text{ for all } \phi \in \mathcal{S}.$$

We then introduce the corresponding bilinear form on the product space $\mathcal{S}^* \times \mathcal{S}$, where $\mathcal{S}^* = C([0, \sigma^0], \mathbb{R}^{3*})$, formulated by

$$\langle \psi, \phi \rangle_n = \psi(0)\phi(0) - \int_{-\sigma^0}^{0}\int_{0}^{\varpi} \psi(\theta - \varpi)\,\mathrm{d}\eta_n(\varpi)\,\phi(\theta)\,\mathrm{d}\theta$$

for $\psi \in \mathcal{S}^*$, $\phi \in \mathcal{S}$.

Let M be the eigenspace corresponding to the characteristic roots $\pm i\chi_{n_H}\tau^H$ of System (3.6) with M^* representing its adjoint space. Thereupon, we can decompose $\mathcal{S}$ as

$$\mathcal{S} = M \oplus N,$$

where $N := \{\phi \in \mathcal{S} : \langle \psi, \phi \rangle = 0 \text{ for any } \psi \in M^*\}$. Then, the bases for M and M^* can be respectively selected by

$$\Phi_{n_H}(\varpi) = \left(\varphi_{n_H}(\varpi),\ \overline{\varphi}_{n_H}(\varpi)\right), \Psi_{n_H}(\theta) = \mathrm{col}\left(\psi^{\mathrm{T}}_{n_H}(\theta),\ \overline{\psi}^{\mathrm{T}}_{n_H}(\theta)\right)$$

such that

$$\langle \Phi_{n_H}, \Psi_{n_H} \rangle = I_3.$$

We perform some calculations to yield

$$\varphi_{n_H}(\varpi) = \begin{pmatrix} \varphi^{(1)}_{n_H} \\ \varphi^{(2)}_{n_H} \\ \varphi^{(3)}_{n_H} \end{pmatrix} \mathrm{e}^{i\chi_{n_H}\tau^H\varpi} := \varphi_{n_H}\mathrm{e}^{i\chi_{n_H}\tau^H\varpi},\ \psi_{n_H}(\theta) = \eta_{n_H} \begin{pmatrix} \psi^{(1)}_{n_H} \\ \psi^{(2)}_{n_H} \\ \psi^{(3)}_{n_H} \end{pmatrix} \mathrm{e}^{-i\chi_{n_H}\tau^H\theta} := \psi_{n_H}\mathrm{e}^{-i\chi_{n_H}\tau^H\theta},$$

where

$$\begin{aligned}
\varphi^{(1)}_{n_H} =& 1, \\
\varphi^{(2)}_{n_H} =& \frac{\left(i\chi_{n_H} + \kappa_{11}(\frac{n}{\iota})^2 - a_{11}(\tau^H)\right)\left(i\chi_{n_H} + \kappa_{33}(\frac{n}{\iota})^2\right)}{a_{12}(\tau^H)\left(\kappa_{33}(\frac{n}{\iota})^2 + i\chi_{n_H}\right) + a_{13}(\tau^H)a_{32}(\tau^H)}, \\
\varphi^{(3)}_{n_H} =& \frac{a_{32}(\tau^H)\left(i\chi_{n_H} + \kappa_{11}(\frac{n}{\iota})^2 - a_{11}(\tau^H)\right) + a_{12}(\tau^H)a_{31}(\tau^H)}{a_{12}(\tau^H)\left(\kappa_{33}(\frac{n}{\iota})^2 + i\chi_{n_H}\right) + a_{13}(\tau^H)a_{32}(\tau^H)} \\
\psi^{(1)}_{n_H} =& 1, \\
\psi^{(2)}_{n_H} =& \frac{\left(i\chi_{n_H} + \kappa_{33}(\frac{n}{\iota})^2\right)\left(i\chi_{n_H} + \kappa_{11}(\frac{n}{\iota})^2 - a_{11}(\tau^H)\right) + a_{13}(\tau^H)a_{31}(\tau^H)}{b_{21}(\tau^H)\mathrm{e}^{-i\chi_{n_H}\tau^H}\left(i\chi_{n_H} + \kappa_{33}(\frac{n}{\iota})^2\right) + a_{31}(\tau^H)\left(a_{32}(\tau^H) - \kappa_{23}C^*(\tau^H)(\frac{n}{\iota})^2\mathrm{e}^{-i\varsigma_n\sigma^H}\right)}, \\
\psi^{(3)}_{n_H} =& \frac{\left(i\chi_n + \kappa_{11}(\frac{n}{l})^2 - a_{11}(\tau^H)\right)\left(a_{23}(\tau^H) - \kappa_{23}C^*(\tau^H)(\frac{n}{l})^2\mathrm{e}^{-i\chi_{n_H}\sigma^H}\right) - b_{21}(\tau^H)a_{13}(\tau^H)\mathrm{e}^{-i\chi_{n_H}\tau^H}}{b_{21}(\tau^H)\mathrm{e}^{-i\chi_{n_H}\tau^H}\left(i\chi_{n_H} + \kappa_{33}(\frac{n}{\iota})^2\right) + a_{31}(\tau^H)\left(a_{32}(\tau^H) - \kappa_{23}C^*(\tau^H)(\frac{n}{l})^2\mathrm{e}^{-i\chi_{n_H}\sigma^H}\right)},
\end{aligned}$$

and

$$\begin{aligned}
\frac{1}{\eta_{n_H}} =& 1 + \varphi^{(2)}_{n_H}\psi^{(2)}_{n_H} + \varphi^{(3)}_{n_H}\psi^{(3)}_{n_H} - \sigma^H\psi^{(2)}_{n_H}\varphi^{(3)}_{n_H}\kappa_{23}\left(\frac{n}{\iota}\right)^2\mathrm{e}^{-i\chi_{n_H}\sigma^H} \\
&+ \tau^H\psi^{(2)}_{n_H}b_{21}(\tau^H)\mathrm{e}^{-i\chi_{n_H}\tau^H} + \tau^H\psi^{(2)}_{n_H}\varphi^{(2)}_{n_H}b_{22}(\tau^H)\mathrm{e}^{-i\chi_{n_H}\tau^H}.
\end{aligned}$$

C_1 can be decomposed into the direct sum

$$C_1 = \mathrm{Im}\,(T) \oplus \mathrm{Ker}\,(T),$$

where $T : C_1 \to \mathrm{Im}\,(T)$ is given by

$$T(\varrho) = \Phi_{n_H}(\varpi)\left\langle \Psi_{n_H}(0), \begin{pmatrix} [\varrho(\cdot), \gamma_{n_H}^{(1)}(x)] \\ [\varrho(\cdot), \gamma_{n_H}^{(2)}(x)] \\ [\varrho(\cdot), \gamma_{n_H}^{(3)}(x)] \end{pmatrix} \right\rangle \beta_{n_H}(x).$$

It follows from [37] that we can introduce the following space:

$$C_1^0 = \{\varrho \in C_1 : \dot{\varrho} \in C_1,\ \varrho(0) \in \mathrm{dom}(\kappa\Delta)\}$$

and denote

$$\mathcal{Z}_x = \begin{pmatrix} \mathcal{Z}_1(t)\beta_{n_H}(x) \\ \mathcal{Z}_2(t)\beta_{n_H}(x) \end{pmatrix},$$

as well as $\mathcal{Z} = (\mathcal{Z}_1(t), \mathcal{Z}_2(t))^T$. We can then decompose $\varrho(\varpi) \in C_1^0$ as

$$\varrho(\varpi) = \Phi_{n_H}(\varpi)\mathcal{Z}_x + \mathcal{W}, \quad \mathcal{W} = \begin{pmatrix} \mathcal{W}^{(1)} \\ \mathcal{W}^{(2)} \\ \mathcal{W}^{(3)} \end{pmatrix} \in C_1^0 \cap \mathrm{Ker}\, T := \mathcal{N}.$$

Accordingly, the variables $\mathcal{Z}$ and $\mathcal{W}$ obey the following abstract ordinary differential equations defined on the space $\mathbb{R}^2 \times \ker T$:

$$\begin{cases} \dot{\mathcal{Z}} = J\mathcal{Z} + \Psi_{n_H}(0) \begin{pmatrix} [\widetilde{G}(\Phi_{n_H}(\varpi)\mathcal{Z}_x + \mathcal{W}, \epsilon), \gamma_{n_H}^{(1)}] \\ [\widetilde{G}(\Phi_{n_H}(\varpi)\mathcal{Z}_x + \mathcal{W}, \epsilon), \gamma_{n_H}^{(2)}] \\ [\widetilde{G}(\Phi_{n_H}(\varpi)\mathcal{Z}_x + \mathcal{W}, \epsilon), \gamma_{n_H}^{(3)}] \end{pmatrix}, \\ \dot{\mathcal{W}} = \mathcal{A}_{\mathcal{N}}\mathcal{W} + (I - T)X_0(\varpi)\widetilde{G}(\Phi_{n_H}(\varpi)\mathcal{Z}_x + \mathcal{W}, \epsilon), \end{cases} \tag{3.7}$$

where $J = \mathrm{diag}\{i\chi_{n_H}, -i\chi_{n_H}\}$. $\mathcal{A}_{\mathcal{N}} : \mathcal{N} \to \mathrm{Ker}\, T$ is defined as

$$\mathcal{A}_{\mathcal{N}}\mathcal{W} = \dot{\mathcal{W}} + X_0(\varpi)\left(L_0^{\kappa}(\mathcal{W}) + L(0)(\mathcal{W}) - \dot{\mathcal{W}}(0)\right)$$

with

$$X_0(\varpi) = \begin{cases} 0, & -1 < \varpi < 0, \\ 1, & \varpi = 0. \end{cases}$$

Applying Taylor's formula to $\widetilde{G}$, G, and G^{κ}, we obtain the following expansions:

$$\widetilde{G}(\rho, \epsilon) = \textstyle\sum_{j\geq 2} \frac{1}{j!}\widetilde{G}_j(\rho, \epsilon),$$
$$G(\rho, \epsilon) = \textstyle\sum_{j\geq 2} \frac{1}{j!}G_j(\rho, \epsilon)$$

and

$$G^{\kappa}(\rho, \epsilon) = \frac{1}{2}G_2^{\kappa}(\rho, \epsilon) + \cdots.$$

From (3.4), we derive

$$\begin{aligned} \widetilde{G}_2(\rho, \epsilon) =& 2\epsilon A(\tau^H)\rho(0) + 2\epsilon\tau^H A_{\epsilon}(\tau^H)\rho(0) + 2\epsilon B(\tau^H)\rho(-1) + 2\epsilon\tau^H B_{\epsilon}(\tau^H)\rho(-1) \\ &+ G_2(\rho, \epsilon) + G_2^{\kappa}(\rho, \epsilon) \end{aligned} \tag{3.8}$$

and

$$\begin{aligned}\widetilde{G}_3(\rho,\epsilon) =&3\tau^H A_{\epsilon\epsilon}(\tau^H)\epsilon^2\rho(0) + 6\epsilon^2 A_\epsilon(\tau^H)\rho(0) + 3\tau^H B_{\epsilon\epsilon}(\tau^H)\epsilon^2\rho(-1) + 6\epsilon^2 B_\epsilon(\tau^H)\rho(-1)\\ &+ G_3(\rho,\epsilon) + G_3^{\kappa}(\rho,\epsilon).\end{aligned} \tag{3.9}$$

In particular, setting $\epsilon = 0$ yields

$$\begin{aligned}G_2(\rho,0) =&f_{200}\left(\rho^{(1)}(0)\right)^2 + f_{110}\rho^{(1)}(0)\rho^{(2)}(0) + f_{101}\rho^{(1)}(0)\rho^{(3)}(0)\\ &+ f_{011}\rho^{(2)}(0)\rho^{(3)}(0) + g_{110}\rho^{(1)}(0)\rho^{(2)}(0),\\ G_3(\rho,0) =&(0,0,0)^{\mathrm{T}},\end{aligned}$$

where

$$f_{200} = \begin{pmatrix} -\frac{2r\tau^H}{K} \\ 0 \\ 0 \end{pmatrix}, \qquad f_{110} = 2\begin{pmatrix} -e_1\tau^H \\ 0 \\ 0 \end{pmatrix}, \qquad f_{101} = 2\begin{pmatrix} -e_2\tau^H \\ 0 \\ \varepsilon_2 e_2\tau^H \end{pmatrix},$$

$$f_{011} = 2\begin{pmatrix} 0 \\ -e_3\tau^H \\ e_3\varepsilon_3\tau^H \end{pmatrix}, \quad g_{110} = 2\begin{pmatrix} 0 \\ \varepsilon_1\tau^H e_1 \mathrm{e}^{-\delta_1\tau^H} \\ 0 \end{pmatrix}.$$

Therefore, System (3.7) can be rewritten as

$$\begin{cases} \dot{\mathcal{Z}} = J\mathcal{Z} + \sum\limits_{j\geq 2}\dfrac{1}{j!}g_j^1(\mathcal{Z},\mathcal{W},\epsilon), \\ \dot{\mathcal{W}} = \mathcal{A}_{\mathcal{N}}\mathcal{W} + \sum\limits_{j\geq 2}\dfrac{1}{j!}g_j^2(\mathcal{Z},\mathcal{W},\epsilon), \end{cases}$$

where

$$g_j^1(\mathcal{Z},\mathcal{W},\epsilon) = \Psi_{n_H}(0)\begin{pmatrix} [\widetilde{G}_j(\Phi_{n_H}(\varpi)\mathcal{Z}_x + \mathcal{W},\epsilon),\gamma_{n_H}^{(1)}] \\ [\widetilde{G}_j(\Phi_{n_H}(\varpi)\mathcal{Z}_x + \mathcal{W},\epsilon),\gamma_{n_H}^{(2)}] \\ [\widetilde{G}_j(\Phi_{n_H}(\varpi)\mathcal{Z}_x + \mathcal{W},\epsilon),\gamma_{n_H}^{(3)}] \end{pmatrix}, \tag{3.10}$$

and

$$g_j^2(\mathcal{Z},\mathcal{W},\epsilon) = (I-T)X_0(\varpi)\widetilde{G}_j(\Phi_{n_H}(\varpi)\mathcal{Z}_x + \mathcal{W},\epsilon).$$

We now employ the following near-identity transformation introduced in [37]:

$$(\mathcal{Z},\mathcal{W}) = (\widetilde{\mathcal{Z}},\widetilde{\mathcal{W}}) + \frac{1}{j!}\left(\mathcal{G}_j^1,\mathcal{G}_j^2\right), \quad j\geq 2 \tag{3.11}$$

to carry out the normal form reduction of System (3.4),

$$\dot{\mathcal{Z}} = J\mathcal{Z} + \sum_{j\geq 2}\frac{1}{j!}f_j^1(\mathcal{Z},0,\epsilon).$$

We can deduce from [31] that

$$f_2^1(\mathcal{Z},0,\epsilon)=\mathrm{Proj}_{\mathrm{Ker}(\mathcal{L}_2^1)}g_2^1(\mathcal{Z},0,\epsilon) \tag{3.12}$$

and

$$f_3^1(\mathcal{Z},0,\epsilon)=\mathrm{Proj}_{\mathrm{Ker}(\mathcal{L}_3^1)}\tilde{g}_3^1(\mathcal{Z},0,\epsilon)=\mathrm{Proj}_{\mathcal{S}_3}\tilde{g}_3^1(\mathcal{Z},0,0)+O(|\epsilon|^2|\mathcal{Z}|), \tag{3.13}$$

where $\tilde{g}_3^1(\mathcal{Z},0,\epsilon)$ is the third-degree homogeneous term in $(\mathcal{Z},\epsilon)$ deduced by the second-order coordinate transformation associated with (3.11). The respective bases of $\ker\mathcal{L}_2^1$ and $\ker\mathcal{L}_3^1$ are given by

$$\mathrm{Ker}(\mathcal{L}_2^1)=\mathrm{Span}\left\{\begin{pmatrix}\epsilon\mathcal{Z}_1\\0\end{pmatrix},\begin{pmatrix}0\\\epsilon\mathcal{Z}_2\end{pmatrix}\right\},$$

$$\mathrm{Ker}(\mathcal{L}_3^1)=\mathrm{Span}\left\{\begin{pmatrix}\mathcal{Z}_1^2\mathcal{Z}_2\\0\end{pmatrix},\begin{pmatrix}\mathcal{Z}_1\epsilon^2\\0\end{pmatrix},\begin{pmatrix}0\\\mathcal{Z}_1\mathcal{Z}_2^2\end{pmatrix}\begin{pmatrix}0\\\mathcal{Z}_2\epsilon^2\end{pmatrix}\right\},$$

and

$$\mathcal{S}_3=\mathrm{Span}\left\{\begin{pmatrix}\mathcal{Z}_1^2\mathcal{Z}_2\\0\end{pmatrix},\begin{pmatrix}0\\\mathcal{Z}_1\mathcal{Z}_2^2\end{pmatrix}\right\}.$$

Throughout the following, we employ the following notation:

$$\mathcal{B}\left(c\mathcal{Z}_1^{\nu_1}\mathcal{Z}_2^{\nu_2}\epsilon\right)=\begin{pmatrix}c\mathcal{Z}_1^{\nu_1}\mathcal{Z}_2^{\nu_2}\epsilon\\\bar{c}\mathcal{Z}_1^{\nu_2}\mathcal{Z}_2^{\nu_1}\epsilon\end{pmatrix},\quad c\in\mathbb{C}.$$

3.1. Second-order term derivation in the normal form

We devote our attention to the explicit form of $f_2^1(\mathcal{Z},0,\epsilon)$ in (3.12). We can deduce from (3.10) that

$$f_2^1(\mathcal{Z},0,\epsilon)=\Psi_{n_H}(0)\begin{pmatrix}[\widetilde{G}_2(\Phi_{n_H}(\varpi)\mathcal{Z}_x+\mathcal{W},\epsilon),\gamma_{n_H}^{(1)}]\\[\widetilde{G}_2(\Phi_{n_H}(\varpi)\mathcal{Z}_x+\mathcal{W},\epsilon),\gamma_{n_H}^{(2)}]\\[\widetilde{G}_2(\Phi_{n_H}(\varpi)\mathcal{Z}_x+\mathcal{W},\epsilon),\gamma_{n_H}^{(3)}]\end{pmatrix}. \tag{3.14}$$

It follows from (3.8) that

$$\begin{aligned}\widetilde{G}_2(\Phi_{n_H}(\varpi)\mathcal{Z}_x,\epsilon)=&2\epsilon A(\tau^H)\Phi_{n_H}(0)\mathcal{Z}_x+2\epsilon\tau^H A_\epsilon(\tau^H)\Phi_{n_H}(0)\mathcal{Z}_x+2\epsilon B(\tau^H)\Phi_{n_H}(-1)\mathcal{Z}_x\\&+2\epsilon\tau^H B_\epsilon(\tau^H)\Phi_{n_H}(-1)\mathcal{Z}_x+G_2(\Phi_{n_H}(\varpi)\mathcal{Z}_x,\epsilon)+G_2^\kappa(\Phi_{n_H}(\varpi)\mathcal{Z}_x,\epsilon).\end{aligned} \tag{3.15}$$

Combining (3.14)-(3.15) and recognizing that

$$[\beta_{n_i}(x),\beta_{n_j}(x)]=\begin{cases}1, & i=j,\\0, & i\neq j,\end{cases}$$

we derive

$$f_2^1(\mathcal{Z},0,\epsilon)=\mathrm{Proj}_{\ker\mathcal{L}_2^1}g_2^1(\mathcal{Z},0,\epsilon)=\mathcal{B}\left(\mathcal{N}^2\mathcal{Z}_1^1\epsilon\right)$$

with

$$\begin{aligned}\mathcal{N}^2=2\psi_{n_H}^{\mathrm{T}}(0)\Big[&A(\tau^H)\varphi_{n_H}(0)+A_\epsilon(\tau^H)\tau^H\varphi_{n_H}(0)+B(\tau^H)\varphi_{n_H}(-1)+B_{\epsilon_1}(\tau^H)\tau^H\varphi_{n_H}(-1)\\&-\left(\frac{n}{\iota}\right)^2\left(\kappa_0\varphi_{n_H}(0)+\varphi_{n_H}(-\sigma^0)\left(\kappa(\tau^H)+\tau^H\kappa_\epsilon(\tau^H)+i\chi_{n_H}\sigma^H\kappa(\tau^H)\right)\right)\Big].\end{aligned}$$

3.2. Third-order term derivation in the normal form

We next derive the explicit representation of $f_3^1(\mathcal{Z},0,\epsilon)$ appearing in Eq (3.13). For this purpose, we employ the notation introduced in [31], which is summarized below:

$$g_2^{(1,1)}(\mathcal{Z},\mathcal{W},0)=\Psi_{n_H}(0)\begin{pmatrix}[\widetilde{G}_2(\Phi_{n_H}(\varpi)\mathcal{Z}_x+\mathcal{W},0),\beta_{n_H}^{(1)}]\\ [\widetilde{G}_2(\Phi_{n_H}(\varpi)\mathcal{Z}_x+\mathcal{W},0),\beta_{n_H}^{(2)}]\\ [\widetilde{G}_2(\Phi_{n_H}(\varpi)\mathcal{Z}_x+\mathcal{W},0),\beta_{n_H}^{(3)}]\end{pmatrix}$$

and

$$g_2^{(1,1)}(\mathcal{Z},\mathcal{W},0)=\Psi_{n_H}(0)\begin{pmatrix}[\widetilde{G}_2^{\kappa}(\Phi_{n_H}(\varpi)\mathcal{Z}_x+\mathcal{W},0),\beta_{n_H}^{(1)}]\\ [\widetilde{G}_2^{\kappa}(\Phi_{n_H}(\varpi)\mathcal{Z}_x+\mathcal{W},0),\beta_{n_H}^{(2)}]\\ [\widetilde{G}_2^{\kappa}(\Phi_{n_H}(\varpi)\mathcal{Z}_x+\mathcal{W},0),\beta_{n_H}^{(3)}]\end{pmatrix}.$$

It follows from [31] that

$$\begin{aligned}\tilde{g}_3^1(\mathcal{Z},0,0)=g_3^1(\mathcal{Z},0,0)+\frac{3}{2}\Big(&\mathrm{D}_{\mathcal{Z}}g_2^1(\mathcal{Z},0,0)\,\mathcal{G}_2^1(\mathcal{Z},0)+\mathrm{D}_{\mathcal{W}}g_2^{(1,1)}(\mathcal{Z},0,0)\,\mathcal{G}_2^2(\mathcal{Z},0)(\varpi)\\&+\mathrm{D}_{\mathcal{W},\mathcal{W}_x,\mathcal{W}_{xx}}g_2^{(1,2)}(\mathcal{Z},0,0)\,\mathcal{G}_2^{2,\kappa}(\mathcal{Z},0)(\varpi)\Big),\end{aligned}$$

where $g_2^1(\mathcal{Z},0,0)=g_2^{(1,1)}(\mathcal{Z},0,0)+g_2^{(1,2)}(\mathcal{Z},0,0)$, and

$$\begin{aligned}\mathrm{D}_{\mathcal{W},\mathcal{W}_x,\mathcal{W}_{xx}}g_2^{(1,2)}(\mathcal{Z},0,0)=&\Big(\mathrm{D}_{\mathcal{W}}g_2^{(1,2)},\ \mathrm{D}_{\mathcal{W}_x}g_2^{(1,2)},\ \mathrm{D}_{\mathcal{W}_{xx}}g_2^{(1,2)}\Big)(\mathcal{Z},0,0),\\ \mathcal{G}_2^1(\mathcal{Z},0)=&(\mathcal{L}_2^1)^{-1}\mathrm{Proj}_{\mathrm{Im}(\mathcal{L}_2^1)}h_2^1(Z,0,0),\\ \mathcal{G}_2^2(\mathcal{Z},0)(\varpi)=&(\mathcal{L}_2^2)^{-1}\mathrm{Proj}_{\mathrm{Im}(\mathcal{L}_2^2)}h_2^2(Z,0,0),\\ \mathcal{G}_2^{2,\kappa}(\mathcal{Z},0)(\varpi)=&\mathrm{col}\Big(\mathcal{G}_2^2(\mathcal{Z},0)(\varpi),\ \mathcal{G}_{2x}^2(\mathcal{Z},0)(\varpi),\ \mathcal{G}_{2xx}^2(\mathcal{Z},0)(\varpi)\Big).\end{aligned}$$

To obtain an explicit expression for $\mathrm{Proj}_{S_3}\tilde{g}_3^1(\mathcal{Z},0,0)$, we divide the calculation into four steps.

Step 1. Calculation of $\mathrm{Proj}_{S_3}g_3^1(\mathcal{Z},0,0)$.

$\widetilde{G}_3(\Phi_{n_H}(\omega)\mathcal{Z}_x,0)$ can be rewritten as

$$\widetilde{G}_3(\Phi_{n_H}(\omega)\mathcal{Z}_x,0)=\sum_{\nu_1+\nu_2=3}\mathcal{E}_{\nu_1\nu_2}\beta_{n_H}^3(x)\mathcal{Z}_1^{\nu_1}\mathcal{Z}_2^{\nu_2}\tag{3.16}$$

with

$$\mathcal{E}_{\nu_1\nu_2}=(0,0,0)^{\mathrm{T}},\ \nu_1+\nu_2=3.$$

From (3.7) together with (3.16), it follows that

$$g_3^1(\mathcal{Z},0,0)=\Phi_{n_H}(0)\Big(\ \textstyle\sum_{\nu_1+\nu_2=3}\mathcal{E}_{\nu_1\nu_2}\int_0^{\iota\pi}\beta_{n_H}^4(x)\mathrm{d}x\mathcal{Z}_1^{\nu_1}\mathcal{Z}_2^{\nu_2}\ \Big).$$

We can then deduce from

$$\int_0^{\iota\pi}\beta_{n_H}^4(x)\mathrm{d}x=\begin{cases}\frac{3}{2l\pi}, & n_H\neq 0,\\ \frac{1}{l\pi}, & n_H=0\end{cases}$$

that

$$\mathrm{Proj}_{\mathcal{S}_3} g_3^1(\mathcal{Z},0,0) = \mathcal{B}\left(\mathcal{N}_1^3 \mathcal{Z}_1^2 \mathcal{Z}_2\right)$$

with

$$\mathcal{N}_1^3 = \begin{cases} \frac{3}{2\iota\pi}\psi_{n_H}^{\mathrm{T}}\mathcal{E}_{21}, & n_H \neq 0, \\ \frac{3}{\iota\pi}\psi_{n_H}^{\mathrm{T}}\mathcal{E}_{21}, & n_H = 0. \end{cases}$$

Step 2. Calculation of $\mathrm{Proj}_{\mathcal{S}_3}\mathrm{D}_{\mathcal{Z}} g_2^1(\mathcal{Z},0,0)\,\mathcal{G}_2^1(\mathcal{Z},0)$.

It follows from (3.3) and (3.9) that

$$\widetilde{G}_2(\Phi_{n_H}(\varpi)\mathcal{Z}_x,0) = G_2(\Phi_{n_H}(\varpi)\mathcal{Z}_x,0) + G_2^{\kappa}(\Phi_{n_H}(\varpi)\mathcal{Z}_x,0).$$

Furthermore, we have

$$\begin{aligned} G_2(\Phi_{n_H}(\varpi)\mathcal{Z}_x + \mathcal{W},\epsilon) &= G_2(\Phi_{n_H}(\varpi)\mathcal{Z}_x + \mathcal{W},0) \\ &= \beta_{n_H}^2(x)\left(\sum_{\nu_1+\nu_2=2} \mathcal{E}_{\nu_1\nu_2}\mathcal{Z}_1^{\nu_1}\mathcal{Z}_2^{\nu_2}\right) + \mathcal{T}_2(\Phi_{n_H}(\varpi)\mathcal{Z}_x,\mathcal{W}) + O(|\mathcal{W}|^2), \end{aligned}$$

where

$$\begin{aligned} \mathcal{E}_{20} =& f_{011}\varphi_{n_H}^{(2)}(0)\varphi_{n_H}^{(3)}(0) + f_{101}\varphi_{n_H}^{(1)}(0)\varphi_{n_H}^{(3)}(0) + f_{110}\varphi_{n_H}^{(1)}(0)\varphi_{n_H}^{(2)}(0) \\ &+ f_{200}(\varphi_{n_H}^{(1)}(0))^2 + g_{110}\varphi_{n_H}^{(1)}(-1)\varphi_{n_H}^{(2)}(-1), \\ \mathcal{E}_{11} =& f_{011}\overline{\varphi_{n_H}^{(2)}(0)}\varphi_{n_H}^{(3)}(0) + f_{110}\varphi_{n_H}^{(1)}(0)\overline{\varphi_{n_H}^{(2)}(0)} + f_{011}\varphi_{n_H}^{(2)}(0)\overline{\varphi_{n_H}^{(3)}(0)} \\ &+ f_{101}\varphi_{n_H}^{(1)}(0)\overline{\varphi_{n_H}^{(3)}(0)} + f_{101}\overline{\varphi_{n_H}^{(1)}(0)}\varphi_{n_H}^{(3)}(0) + f_{110}\overline{\varphi_{n_H}^{(1)}(0)}\varphi_{n_H}^{(2)}(0) \\ &+ 2f_{200}\varphi_{n_H}^{(1)}(0)\overline{\varphi_{n_H}^{(1)}(0)} + g_{110}\overline{\varphi_{n_H}^{(1)}(-1)}\varphi_{n_H}^{(2)}(-1) + g_{110}\varphi_{n_H}^{(1)}(-1)\overline{\varphi_{n_H}^{(2)}(-1)}, \\ \mathcal{E}_{02} =& f_{011}\overline{\varphi_{n_H}^{(2)}(0)\varphi_{n_H}^{(3)}(0)} + f_{101}\overline{\varphi_{n_H}^{(1)}(0)\varphi_{n_H}^{(3)}(0)} + f_{110}\overline{\varphi_{n_H}^{(1)}(0)\varphi_{n_H}^{(2)}(0)} \\ &+ f_{200}\overline{(\varphi_{n_H}^{(1)}(0))^2} + g_{110}\overline{\varphi_{n_H}^{(1)}(-1)\varphi_{n_H}^{(2)}(-1)}, \end{aligned}$$

and

$$\begin{aligned} \mathcal{T}_2(\Phi_{n_H}(\varpi)\mathcal{Z}_x,\mathcal{W}) =& \Big[\left(f_{011}\varphi_{n_H}^{(3)}(0) + f_{110}\varphi_{n_H}^{(1)}(0)\right)\mathcal{W}^{(2)}(0) + \left(f_{011}\varphi_{n_H}^{(2)}(0) + f_{101}\varphi_{n_H}^{(1)}(0)\right)\mathcal{W}^{(3)}(0) \\ &+ \left(f_{110}\varphi_{n_H}^{(2)}(0) + f_{101}\varphi_{n_H}^{(3)}(0) + 2f_{200}\varphi_{n_H}^{(1)}(0)\right)\mathcal{W}^{(1)}(0) \\ &+ g_{110}\varphi_{n_H}^{(2)}(-1)\mathcal{W}^{(1)}(-1) + g_{110}\varphi_{n_H}^{(2)}(-1)\mathcal{W}^{(2)}(-1)\Big]\mathcal{Z}_1\beta(x) \\ &+ \Big[\left(f_{011}\overline{\varphi_{n_H}^{(3)}(0)} + f_{110}\overline{\varphi_{n_H}^{(1)}(0)}\right)\mathcal{W}^{(2)}(0) + \left(f_{011}\overline{\varphi_{n_H}^{(2)}(0)} + f_{101}\overline{\varphi_{n_H}^{(1)}(0)}\right)\mathcal{W}^{(3)}(0) \\ &+ \left(f_{110}\overline{\varphi_{n_H}^{(2)}(0)} + f_{101}\overline{\varphi_{n_H}^{(3)}(0)} + 2f_{200}\overline{\varphi_{n_H}^{(1)}(0)}\right)\mathcal{W}^{(1)}(0) \\ &+ g_{110}\overline{\varphi_{n_H}^{(2)}(-1)}\mathcal{W}^{(1)}(-1) + g_{110}\overline{\varphi_{n_H}^{(2)}(-1)}\mathcal{W}^{(2)}(-1)\Big]\mathcal{Z}_2\beta(x). \end{aligned}$$

We can also obtain

$$G_2^{\kappa}(\Phi_{n_H}(\varpi)\mathcal{Z}_x,0)=\left(\frac{n_H}{\iota}\right)^2\left(\tilde{\beta}_{n_H}^2(x)-\beta_{n_H}^2(x)\right)\left(\sum_{\nu_1+\nu_2=2}\mathcal{E}_{\nu_1\nu_2}^{\kappa}\mathcal{Z}_1^{\nu_1}\mathcal{Z}_2^{\nu_2}\right),$$

with $\tilde{\beta}_{n_H}^2(x)=\sqrt{2}/\sqrt{\iota\pi}\sin(n_Hx/\iota)$ and

$$\mathcal{E}_{20}^{\kappa}=2\kappa_{23}\tau^H\begin{pmatrix}0\\ \varphi^{(2)}(0)\varphi^{(3)}(-\sigma^0)\\ 0\end{pmatrix}=\overline{\mathcal{E}_{02}^{\kappa}},$$

$$\mathcal{E}_{11}^{\kappa}=2\kappa_{23}\tau^H\begin{pmatrix}0\\ 2\Re\{\overline{\varphi^{(2)}(0)}\varphi^{(3)}(-\sigma^0)\}\\ 0\end{pmatrix}.$$

In light of

$$\int_0^{\iota\pi}\tilde{\beta}_{n_H}(x)\beta_{n_H}(x)\mathrm{d}x=\begin{cases}0, & n_H\neq 0,\\ 0, & n_H=0,\end{cases}\quad\int_0^{\iota\pi}\beta_{n_H}^3(x)\mathrm{d}x=\begin{cases}0, & n_H\neq 0,\\ \frac{1}{\sqrt{\iota\pi}}, & n_H=0,\end{cases}$$

we have

$$\mathrm{Proj}_{\mathcal{S}_3}\mathrm{D}_{\mathcal{Z}}g_2^1(\mathcal{Z},0,0)\,\mathcal{G}_2^1(\mathcal{Z},0)=\mathcal{B}\left(\mathcal{N}_2^3\mathcal{Z}_1^2\mathcal{Z}_2\right)$$

with

$$\mathcal{N}_2^3=\begin{cases}0, & n_H\neq 0,\\ \frac{1}{\iota\pi i\chi_{n_H}\tau^H}\left(-(\psi_{n_H}^{\mathrm{T}}\mathcal{E}_{20})(\psi_{n_H}^{\mathrm{T}}\mathcal{E}_{11})+|\psi_{n_H}^{\mathrm{T}}\mathcal{E}_{20}|^2+\frac{2}{3}|\psi_{n_H}^{\mathrm{T}}\mathcal{E}_{02}|^2\right), & n_H=0.\end{cases}$$

Step 3. The calculation of $\mathrm{Proj}_{\mathcal{S}_3}(\mathrm{D}_{\mathcal{W}}g_2^{(1,1)}(\mathcal{Z},0,0)\,\mathcal{G}_2^2(\mathcal{Z},0)(\varpi))$.

Denote

$$\mathcal{G}_2^2(\mathcal{Z},0)(\varpi)=\mathfrak{g}(\mathcal{Z},\varpi)=\sum_{n\in\mathbb{N}_0}\mathfrak{g}_n(\mathcal{Z},\varpi)\beta_n(x),$$

where $\mathfrak{g}_n(\mathcal{Z},\varpi)=\sum_{\nu_1+\nu_2=2}\mathfrak{g}_{n,\nu_1\nu_2}(\varpi)\mathcal{Z}_1^{\nu_1}\mathcal{Z}_2^{\nu_2}$. It follows from [31] that

$$\begin{pmatrix}[\mathcal{T}_2(\Phi_{n_H}(\varpi)\mathcal{Z}_x,\sum_{n\in\mathbb{N}_0}\mathfrak{g}_n(\mathcal{Z},\varpi)\beta_n(x)),\gamma_n^{(1)}]\\ [\mathcal{T}_2(\Phi_{n_H}(\varpi)\mathcal{Z}_x,\sum_{n\in\mathbb{N}_0}\mathfrak{g}_n(\mathcal{Z},\varpi)\beta_n(x)),\gamma_n^{(2)}]\\ [\mathcal{T}_2(\Phi_{n_H}(\varpi)\mathcal{Z}_x,\sum_{n\in\mathbb{N}_0}\mathfrak{g}_n(\mathcal{Z},\varpi)\beta_n(x)),\gamma_n^{(3)}]\end{pmatrix}$$

$$=\sum_{n\in\mathbb{N}_0}\breve{\beta}_n\left(\mathcal{T}_2(\varphi_{n_H}(\varpi)\mathcal{Z}_1,\mathfrak{g}_n(\mathcal{Z},\varpi))+\mathcal{T}_2(\overline{\varphi}_{n_H}(\varpi)\mathcal{Z}_2,\mathfrak{g}_n(\mathcal{Z},\varpi))\right),$$

where

$$\breve{\beta}_n=\begin{cases}\int_0^{\iota\pi}\beta_{n_H}^2(x)\beta_n(x)=\begin{cases}\frac{1}{\sqrt{\iota\pi}}, & n=0,\\ \frac{1}{\sqrt{2\iota\pi}}, & n=2n_H,\quad n_H\neq 0\\ 0, & \text{otherwise},\end{cases}\\ \int_0^{\iota\pi}\beta_{n_H}^2(x)\beta_n(x)=\begin{cases}\frac{1}{\sqrt{\iota\pi}}, & n=0,\\ 0, & n\neq 0,\end{cases}\quad n_H=0.\end{cases}$$

Therefore, we have

$$\begin{aligned}&\mathrm{D}_{\mathcal{W}} g_2^{(1,1)}(\mathcal{Z},0,0)\,\mathcal{G}_2^2(\mathcal{Z},0)(\varpi)\\ =&\Psi_{n_H}(0)\left(\sum_{n=0,n=2n_H}\breve{\beta}_n\Big(\mathcal{T}_2(\varphi_{n_H}(\varpi)\mathcal{Z}_1,\mathfrak{g}_n(\mathcal{Z},\varpi))+\mathcal{T}_2(\overline{\varphi}_{n_H}(\varpi)\mathcal{Z}_2,\mathfrak{g}_n(\mathcal{Z},\varpi))\Big)\right),\end{aligned}$$

and

$$\mathrm{Proj}_S(\mathrm{D}_{\mathcal{W}} g_2^{(1,1)}(\mathcal{Z},0,0)\,\mathcal{G}_2^2(\mathcal{Z},0)(\varpi))=\mathcal{B}\left(\mathcal{N}_3^3\mathcal{Z}_1^2\mathcal{Z}_2\right),$$

where

$$\mathcal{N}_3^3=\begin{cases}\frac{1}{\sqrt{l\pi}}\psi^{\mathrm{T}}\left(\mathcal{T}_2(\varphi_{n_H}(\varpi),\mathfrak{g}_{0,11}(\varpi))+\mathcal{T}_2(\overline{\varphi}_{n_H}(\varpi),\mathfrak{g}_{0,20}(\varpi))\right)\\ +\frac{1}{\sqrt{2l\pi}}\psi^{\mathrm{T}}\left(\mathcal{T}_2(\varphi_{n_H}(\varpi),\mathfrak{g}_{2n_H,11}(\varpi))+\mathcal{T}_2(\overline{\varphi}_{n_H}(\varpi),\mathfrak{g}_{2n_H,20}(\varpi))\right),\ n_H\neq 0,\\ \frac{1}{\sqrt{l\pi}}\psi^{\mathrm{T}}\left(\mathcal{T}_2(\varphi_{n_H}(\varpi),\mathfrak{g}_{0,11}(\varpi))+\mathcal{T}_2(\overline{\varphi}_{n_H}(\varpi),\mathfrak{g}_{0,20}(\varpi))\right),\ n_H=0.\end{cases}\tag{3.17}$$

Next, we present the formulae of $\mathfrak{g}_{0,20}(\varpi)$, $\mathfrak{g}_{0,11}(\varpi)$, $\mathfrak{g}_{2n,20}(\varpi)$, and $\mathfrak{g}_{2n,11}(\varpi)$ in (3.17). Denote

$$\widetilde{\mathcal{E}}_{\nu_1\nu_2}=\mathcal{E}_{\nu_1\nu_2}-2\left(\tfrac{n}{\iota}\right)^2\mathcal{E}^{\kappa}_{\nu_1\nu_2},\ \nu_1,\nu_2=0,1,2,\ \nu_1+\nu_1=2$$

and

$$\mathcal{L}(\lambda;n)=\lambda I_3+\tau^H\left(\tfrac{n}{\iota}\right)^2\kappa_0+\tau^H\left(\tfrac{n}{\iota}\right)^2\kappa(\tau^H)\mathrm{e}^{-\lambda\sigma^0}-\tau^H A(\tau^H)-\tau^H B(\sigma^H)\mathrm{e}^{-\lambda}.$$

We can deduce from [38, 39] that

$$\mathfrak{g}_{0,20}(\varpi)=\begin{cases}\frac{1}{\sqrt{\iota\pi}}(\mathcal{L}(2i\chi_{n_H}\tau^H;0))^{-1}\mathcal{E}_{20}\mathrm{e}^{2i\chi_{n_H}\tau^H\varpi}, & n_H\neq 0,\\ \frac{1}{\sqrt{\iota\pi}}\mathrm{e}^{2i\chi_{n_H}\tau^H\varpi}\int_0^{\varpi}\Phi_{n_H}(t)\Psi_{n_H}(0)\mathcal{E}_{20}\mathrm{e}^{-2i\chi_{n_H}\tau^H t}\mathrm{d}t+C_1\mathrm{e}^{2i\chi_{n_H}\tau^H\varpi}, & n_H=0,\end{cases}$$

$$\mathfrak{g}_{0,11}(\varpi)=\begin{cases}\frac{1}{\sqrt{\iota\pi}}(\mathcal{L}(0;0))^{-1}\mathcal{E}_{11}, & n_H\neq 0,\\ \frac{1}{\sqrt{\iota\pi}}\int_0^{\varpi}\Phi_{n_H}(t)\Psi_{n_H}(0)\mathcal{E}_{11}\mathrm{d}t+C_2, & n_H=0,\end{cases}$$

$$\mathfrak{g}_{2n_H,20}(\varpi)=\begin{cases}\frac{1}{\sqrt{2\iota\pi}}(\mathcal{L}(2i\chi_{n_H}\tau^H;2n_H))^{-1}\widetilde{\mathcal{E}}_{20}\mathrm{e}^{2i\chi_{n_H}\tau^H\varpi}, & n_H\neq 0,\\ (0,0,0)^{\mathrm{T}}, & n_H=0,\end{cases}$$

$$\mathfrak{g}_{2n_H,11}(\varpi)=\begin{cases}\frac{1}{\sqrt{2\iota\pi}}(\mathcal{L}(0;2n_H))^{-1}\widetilde{\mathcal{E}}_{11}, & n_H\neq 0,\\ (0,0,0)^{\mathrm{T}}, & n_H=0,\end{cases}$$

with

$$\begin{aligned}C_1=&(\mathcal{L}(2i\chi_{n_H}\tau^H;0))^{-1}\left(\left(\frac{1}{\sqrt{\iota\pi}}-\frac{1}{\sqrt{\iota\pi}}\Phi_{n_H}(0)\Psi_{n_H}(0)\right)\mathcal{E}_{20}\right.\\ &\left.-\tau^H B(\sigma^H)\frac{1}{\sqrt{\iota\pi}}\mathrm{e}^{-2i\chi_{n_H}\tau^H}\int_{-1}^{0}\Phi_{n_H}(t)\Psi_{n_H}(0)\mathcal{E}_{20}\mathrm{e}^{-2i\chi_{n_H}\tau^H t}\mathrm{d}t\right),\\ C_2=&(\mathcal{L}(0;0))^{-1}\left(\frac{1}{\sqrt{\iota\pi}}\mathcal{E}_{11}-\frac{1}{\sqrt{\iota\pi}}\Phi_{n_H}(0)\Psi_{n_H}(0)\mathcal{E}_{11}-\frac{1}{\sqrt{\iota\pi}}\tau^H B(\sigma^H)\int_{-1}^{0}\Phi_{n_H}(t)\Psi_{n_H}(0)\mathcal{E}_{11}\right).\end{aligned}$$

Step 4. The calculation of $\mathrm{Proj}_{\mathcal{S}_3}(\mathrm{D}_{\mathcal{W},\mathcal{W}_x,\mathcal{W}_{xx}} g_2^{(1,2)}(\mathcal{Z},0,0)\,\mathcal{G}_2^{2,\kappa}(\mathcal{Z},0)(\varpi))$.

Denote $\varrho(\varpi) = (\varrho^{(1)}, \varrho^{(2)}, \varrho^{(3)}) = \Phi_{n_H}(\varpi)\mathcal{Z}_x$ and

$$\begin{aligned} G_2^{\kappa}(\varrho(\varpi), \mathcal{W}, \mathcal{W}_x, \mathcal{W}_{xx}) &= G_2^{\kappa}(\varrho(\varpi) + \mathcal{W}, 0) \\ &= 2\kappa_{23}\tau^H \begin{pmatrix} 0 \\ (\varrho^{(2)}(0) + \mathcal{W}^{(2)}(0))(\varrho_{xx}^{(3)}(-\sigma^0) + \mathcal{W}_{xx}^{(3)}(-\sigma^0)) \\ 0 \end{pmatrix} \\ &\quad + 2\kappa_{23}\tau^H \begin{pmatrix} 0 \\ (\varrho_x^{(2)}(0) + \mathcal{W}_x^{(2)}(0))(\varrho_x^{(3)}(-\sigma^0) + \mathcal{W}_x^{(2)}(-\sigma^0)) \\ 0 \end{pmatrix} \end{aligned}$$

as well as

$$\begin{cases} \mathcal{T}_2^{(\kappa,1)}(\varphi_{n_H}(\varpi), w(\varpi)) = 2\kappa_{23}\tau^H \begin{pmatrix} 0 \\ w^{(2)}(0)\varphi_{n_H}^{(3)}(-\sigma^0) \\ 0 \end{pmatrix}, \\ \mathcal{T}_2^{(\kappa,2)}(\varphi_{n_H}(\varpi), w(\varpi)) = 2\kappa_{23}\tau^H \begin{pmatrix} w^{(2)}(0)\varphi_{n_H}^{(3)}(-\sigma^0) + w^{(3)}(-\sigma^0)\varphi_{n_H}^{(2)}(0) \\ 0 \end{pmatrix}, \\ \mathcal{T}_2^{(\kappa,2)}(\varphi_{n_H}(\varpi), w(\varpi)) = 2\kappa_{23}\tau^H \begin{pmatrix} 0 \\ w^{(3)}(-\sigma^0)\varphi_{n_H}^{(2)}(0) \\ 0 \end{pmatrix}. \end{cases}$$

Therefore, we can obtain that

$$\mathrm{Proj}_{\mathcal{S}_3}(\mathrm{D}_{\mathcal{W},\mathcal{W}_x,\mathcal{W}_{xx}} g_2^{(1,2)}(\mathcal{Z}, 0, 0)\, \mathcal{G}_2^{2,\kappa}(\mathcal{Z}, 0)(\varpi)) = \mathcal{B}(\mathcal{N}_4^3 \mathcal{Z}_1^2 \mathcal{Z}_2),$$

where

$$\mathcal{N}_4^3 = \begin{cases} -\frac{1}{\sqrt{\iota\pi}}(\frac{n}{\iota})^2 \psi_{n_H}^{\mathrm{T}} \Big(\mathcal{T}_2^{(\kappa,1)}(\varphi_{n_H}(\varpi), \mathfrak{g}_{0,11}(\varpi)) + \mathcal{T}_2^{(\kappa,1)}(\varphi_{n_H}(\varpi), \mathfrak{g}_{0,20}(\varpi))) \Big) & n_H \neq 0, \\ +\frac{1}{\sqrt{2\iota\pi}} \psi^{\mathrm{T}} \sum_{j=1,2,3} \acute{\beta}_{2n_H}^{(j)} \Big(\mathcal{T}_2^{(\kappa,j)}(\varphi_{n_H}(\varpi), \mathfrak{g}_{2n_H,11}(\varpi)) + \mathcal{T}_2^{(\kappa,j)}(\varphi_{n_H}(\varpi), \mathfrak{g}_{2n_H,20}(\varpi)) \Big), \\ 0, \ n_H = 0 \end{cases}$$

with

$$\acute{\beta}_{2n_H}^{(1)} = -\frac{n_H^2}{\iota^2}, \ \acute{\beta}_{2n_H}^{(2)} = 2\frac{n_H^2}{\iota^2}, \ \acute{\beta}_{2n_H}^{(3)} = -\frac{4n_H^2}{\iota^2}.$$

Therefore, we have the explicit formulae of Hopf bifurcation as below:

$$\dot{\mathcal{Z}} = \mathcal{J}\mathcal{Z} + \tfrac{1}{2} \begin{pmatrix} \mathcal{N}_2 \mathcal{Z}_1 \varepsilon \\ \overline{\mathcal{N}_2} \mathcal{Z}_2 \varepsilon \end{pmatrix} + \tfrac{1}{3!} \begin{pmatrix} \mathcal{N}_3 \mathcal{Z}_1^2 \mathcal{Z}_2 \\ \overline{\mathcal{N}_3} \mathcal{Z}_1 \mathcal{Z}_2^2 \end{pmatrix} + O(|\mathcal{Z}|\varepsilon^2 + |\mathcal{Z}|^4),$$

where

$$\mathcal{N}_3 = \mathcal{N}_1^3 + \tfrac{3}{2}\left(\mathcal{N}_2^3 + \mathcal{N}_3^3 + \mathcal{N}_4^3\right).$$

We are therefore led to the following conclusion.

Theorem 2. *A Hopf bifurcation is supercritical (subcritical) whenever* $\Re(\mathcal{N}_2)\Re(\mathcal{N}_3) < 0$ (> 0). *Moreover, the bifurcating periodic orbits are stable (unstable) if* $\Re(\mathcal{N}_3) < 0$ (> 0).

4. Numerical explorations

We conduct some numerical experiments in this section to verify the theoretical predictions and to assess the role of delays in shaping the spatiotemporal patterns of System (1.2). We adopt the parameter values from [14] as

$$r = 1,\ k = 1,\ e_1 = 1,\ e_2 = 1,\ e_3 = 0.6,\ \varepsilon_1 = 2.5, \varepsilon_2 = 0.005,\ \varepsilon_3 = 0.5,$$
$$\delta_1 = 0.1,\ \delta_2 = 0.1,\ \delta_3 = 0.01.$$

The remaining parameters are chosen for illustrative purposes in the simulations as

$$\kappa_{11} = 0.1,\ \kappa_{22} = 0.05,\ \kappa_{33} = 0.02,\ \kappa_{23} = 1.18,\ \iota = 3.$$

Then, System (1.2) turns into

$$\begin{cases} \dfrac{\partial R}{\partial t} = 0.1R_{xx} + R(1-R) - RC - RP, & x \in (0, 3\pi), \\ \dfrac{\partial C}{\partial t} = 0.05C_{xx} + 1.18(CP_x(x, t-\sigma))_x + 2.5R_\tau C_\tau e^{-0.1\tau} - 0.1C - 0.6CP, & x \in (0, 3\pi), \\ \dfrac{\partial P}{\partial t} = 0.02P_{xx} + 0.005RP + 0.3CP - 0.01P, & x \in (0, 3\pi), \\ R_x(x,t) = C_x(x,t) = P_x(x,t) = 0,\ x = 0,\ 3\pi. \end{cases} \tag{4.1}$$

The unstable interval for τ are $(0.2168, 2.8326)$, as shown in [14] for $n = 0$. We then employ the method developed in Section 2 to generate the crossing curves for $5 \le n \le 7$ as illustrated in Figure 1 because the feasible regions Ω_n are empty in all remaining cases. The yellow-shaded regions correspond to the stable region. We can observe from Figure 1 that the maturation delay τ can exert a stabilizing effect on the system after a finite number of stability switches, whereas the memory delay σ can induce mode–5 Hopf bifurcations.

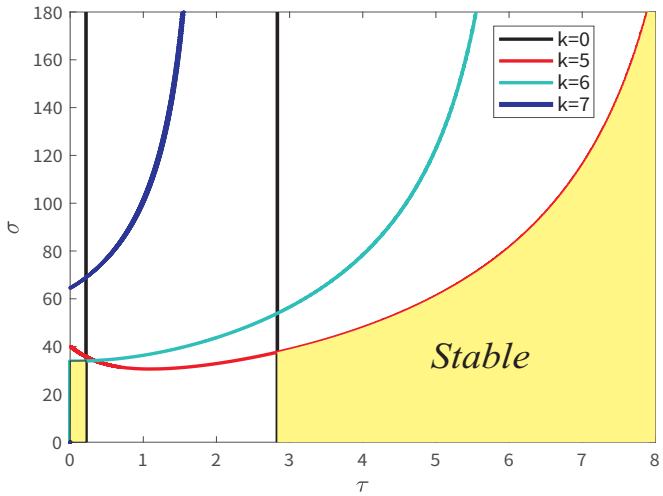

Figure 1. Crossing curves and double Hopf bifurcation point.

For a fixed value of $\sigma^H = 70$, the critical quantities associated with the mode–5 Hopf bifurcation are

$$n_H = 5, \quad \tau^H \approx 5.4957, \quad \chi_{n_H} \approx 0.0343.$$

Applying the algorithms described in Section 3, we further obtain the normal form coefficients

$$\Re(\mathcal{N}_2) \approx -0.0037, \qquad \Re(\mathcal{N}_3) \approx -27.7000.$$

It then follows from Theorem 2 that the mode−5 Hopf bifurcation is subcritical. Consequently, the constant steady state E^* is asymptotically stable for $\tau > \tau^H \approx 5.4957$, whereas for $\tau < \tau^H \approx 5.4957$, stable mode−5 spatially heterogeneous periodic oscillations emerge. The numerical simulations further corroborate this theoretical result, as illustrated in Figures 2 and 3.

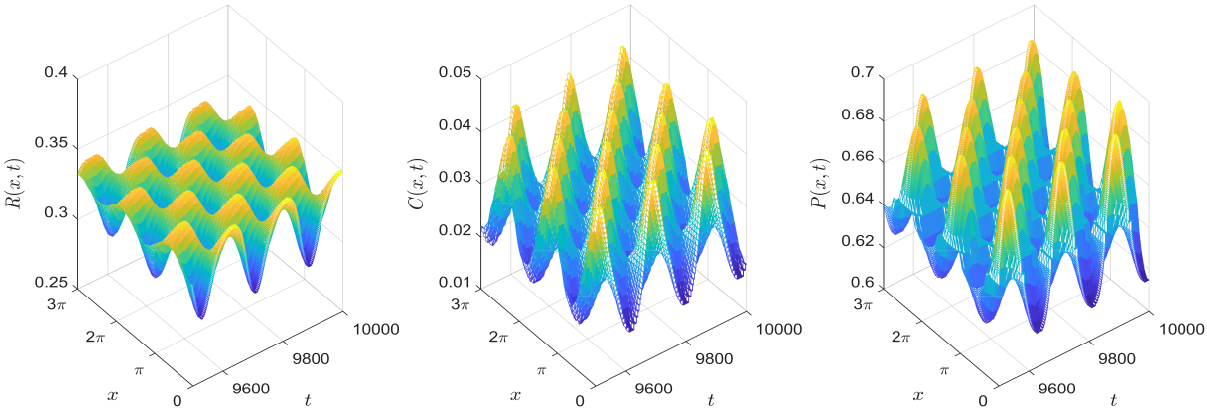

Figure 2. Spatiotemporal dynamics of $R(x,t)$, $C(x,t)$, $P(x,t)$ of System (4.1) with $\sigma^H = 70$, $\tau = 5 < \tau^H \approx 5.4957$, and initial values $(R(x,t), C(x,t), P(x,t)) = E_* + 0.01\cos(5x/3)$.

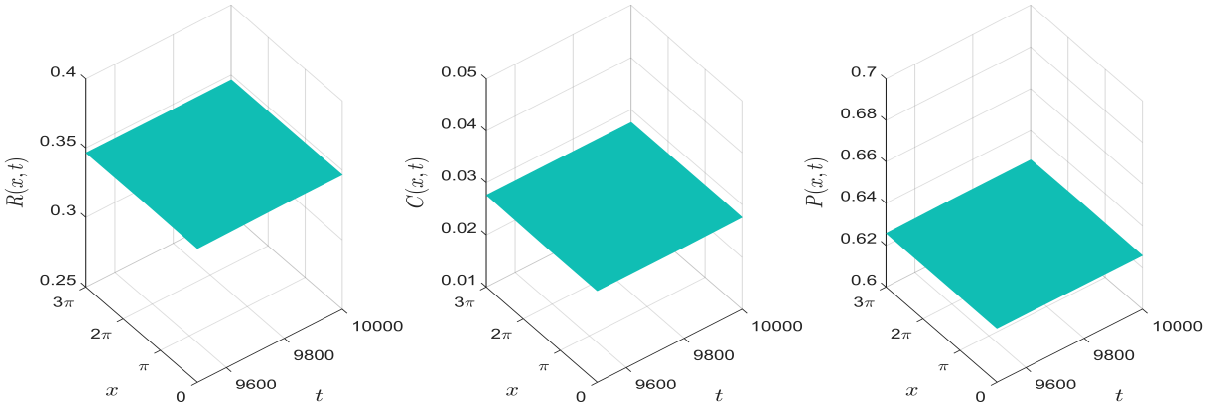

Figure 3. Spatiotemporal dynamics of $R(x,t)$, $C(x,t)$, $P(x,t)$ of System (4.1) with $\sigma^H = 70$, $\tau = 6 > \tau^H \approx 5.4957$, and initial values $(R(x,t), C(x,t), P(x,t)) = E_* + 0.01\cos(5x/3)$.

For $\sigma^H = 20$, the critical quantities corresponding to the mode−0 Hopf bifurcation are

$$n_H = 0, \quad \tau^H \approx 0.2168, \quad \chi_{n_H} \approx 0.1350.$$

Similarly, we obtain

$$\Re(\mathcal{N}_2) \approx 0.0009, \qquad \Re(\mathcal{N}_3) \approx -4.6730.$$

According to Theorem 2, the mode−0 Hopf bifurcation is supercritical. Consequently, E^* is asymptotically stable for $\tau < \tau^H \approx 0.2168$, whereas for $\tau > \tau^H \approx 0.2168$, stable spatially homogeneous periodic oscillations can be observed. This theoretical prediction is again confirmed by the numerical simulations; see Figures 4 and 5.

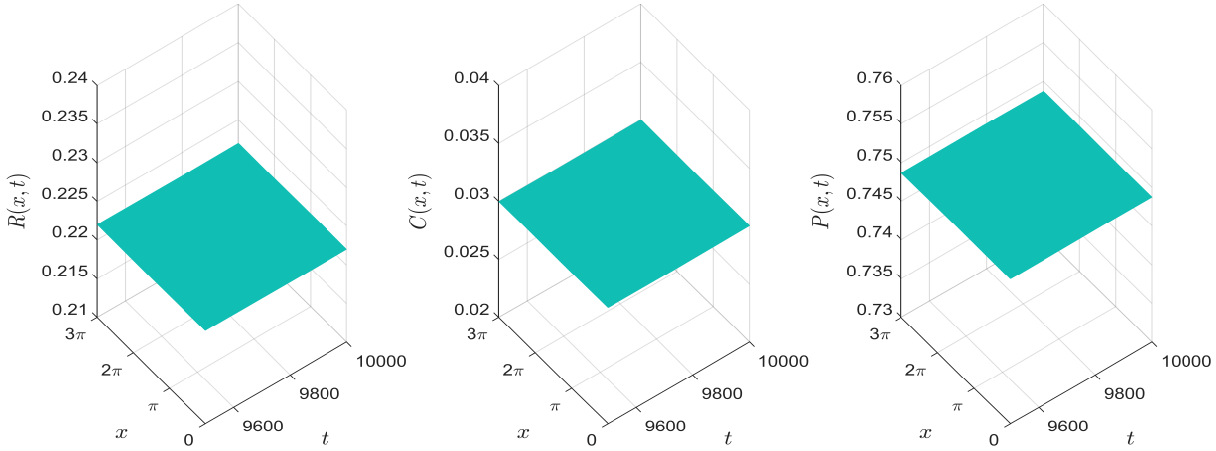

Figure 4. Spatiotemporal dynamics of $R(x,t)$, $C(x,t)$, $P(x,t)$ of System (4.1) with $\sigma^H = 20$, $\tau = 0.1 < \tau^H \approx 0.2168$, and initial values $(R(x,t), C(x,t), P(x,t)) = E_* + 0.01\cos(5x/3)$.

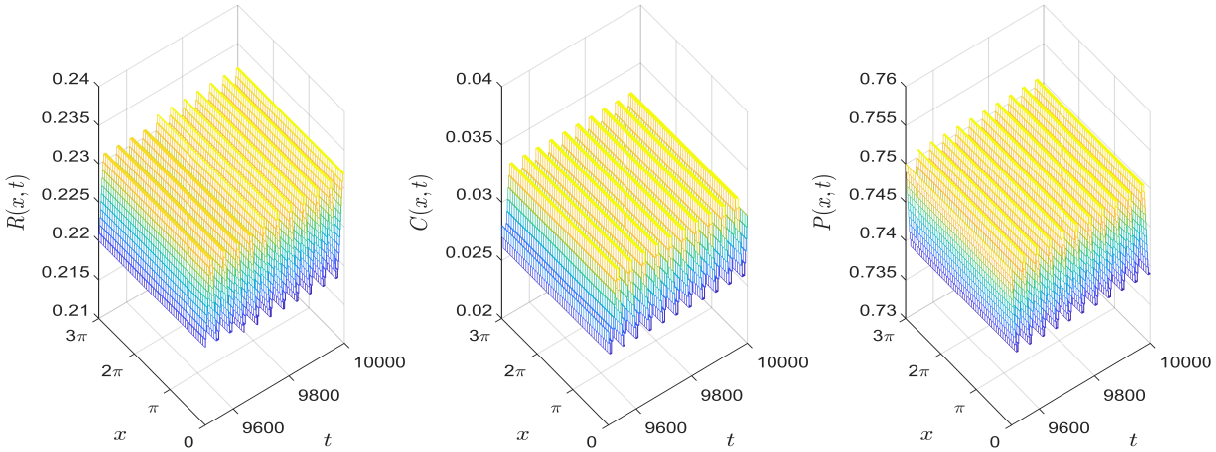

Figure 5. Spatiotemporal dynamics of $R(x,t)$, $C(x,t)$, $P(x,t)$ of System (4.1) with $\sigma^H = 20$, $\tau = 0.3 > \tau^H \approx 0.2168$, and initial values $(R(x,t), C(x,t), P(x,t)) = E_* + 0.01\cos(5x/3)$.

5. Conclusions

In this paper, we investigate the influence of two delays on the spatiotemporal dynamics of a diffusive three−species intraguild predation system. By means of a geometric approach, we determine the stable regions in the (τ, σ)−plane and identify the Hopf bifurcation curves forming their boundaries. We further extend existing normal form techniques to the case where the maturation delay τ serves as

the bifurcation parameter where the system coefficients depend on it, which enables us to determine the bifurcation direction and the stability of the bifurcating periodic orbits. Our results show that, after a finite number of stability switches, the maturation delay τ may play a stabilizing role, whereas the memory delay σ can give rise to mode−5 Hopf bifurcations. The system can exhibit a rich variety of coexistence patterns, including constant steady states, stable spatially homogeneous periodic oscillations, and stable mode−5 spatially heterogeneous periodic oscillations. Some interesting issues warrant further investigation. For example, various uncertainties such as temperature fluctuations can significantly affect predator−prey interactions [40–42]. Analyzing stochastic predator−prey models incorporating time delays and diffusion remains an open and challenging problem.

Author contributions

Shuai Li: Writing−original draft, Methodology, Software. Bing Fang: Visualization, Formal analysis. Xinyu Song: Writing−review, editing. Chengdai Huang: Supervision, Visualization. All authors have read and approved the final version of the manuscript for publication.

Use of Generative-AI tools declaration

The authors declare they have not used Artificial Intelligence (AI) tools in the creation of this article.

Acknowledgments

This work was supported by the National Natural Science Foundation of China (grant number 12401651, 12571548) and the Nanhu Scholars Program for Young Scholars of the Xinyang Normal University.

Conflict of interest

The authors declare no conflicts of interest in this paper.

References

1. S. Gao, H. Wang, S. Yuan, Theory of stoichiometric intraguild predation: algae, ciliate, and daphnia, *Bull. Math. Biol.*, **86** (2024), 79. https://doi.org/10.1007/s11538-024-01306-z
2. C. A. M. Hickerson, C. D. Anthony, B. M. Walton, Edge effects and intraguild predation in native and introduced centipedes: evidence from the field and from laboratory microcosms, *Oecologia*, **146** (2005), 110–119. https://doi.org/10.1007/s00442-005-0197-y
3. P. Morin, Productivity, intraguild predation, and population dynamics in experimental food webs, *Ecology*, **80** (1999), 752–760. https://doi.org/10.1890/0012-9658(1999)080[0752:PIPAPD]2.0.CO;2
4. Y. Kang, L. Wedekin, Dynamics of a intraguild predation model with generalist or specialist predator, *J. Math. Biol.*, **67** (2013), 1227–1259. https://doi.org/10.1007/s00285-012-0584-z

5. G. A. Polis, R. D. Holt, Intraguild predation: the dynamics of complex trophic interactions, *Trends Ecol. Evol.*, **7** (1992), 151–154. https://doi.org/10.1016/0169-5347(92)90208-S

6. R. D. Holt, G. A. Polis, A theoretical framework for intraguild predation, *Amer. Nat.*, **149** (1997), 745–764. https://doi.org/10.1086/286018

7. U. Kumar, P. S. Mandal, Impact of additive Allee effect on the dynamics of an intraguild predation model with specialist predator, *Int. J. Bifurcat. Chaos*, **30** (2020), 2050239. https://doi.org/10.1142/S0218127420502399

8. J. Ji, L. Wang, Competitive exclusion and coexistence in an intraguild predation model with Beddington–DeAngelis functional response, *Commun. Nonlinear Sci. Numer. Simul.*, **107** (2022), 106192. https://doi.org/10.1016/j.cnsns.2021.106192

9. Y. Kuang, *Delay differential equations: with applications in population dynamics*, Academic Press, 1993.

10. S. A. Gourley, Y. Kuang, A stage structured predator-prey model and its dependence on maturation delay and death rate, *J. Math. Biol.*, **49** (2004), 188–200, https://doi.org/10.1007/s00285-004-0278-2

11. H. Shu, X. Hu, L. Wang, J. Watmough, Delay induced stability switch, multitype bistability and chaos in an intraguild predation model, *J. Math. Biol.*, **71** (2015), 1269–1298. https://doi.org/10.1007/s00285-015-0857-4

12. M. Yamaguchi, Y. Takeuchi, W. Ma, Dynamical properties of a stage structured three-species model with intra-guild predation, *J. Comput. Appl. Math.*, **201** (2007), 327–338. https://doi.org/10.1016/j.cam.2005.12.033

13. S. Li, Y. Yang, X. Song, The joint impacts of maturation delay and digestion delay on the dynamics of a predator–prey model, *J. Xinyang Norm. Univ. (Nat. Sci. Ed.)*, **38** (2025), 421–427. https://doi.org/10.3969/j.issn.2097-583X.2025.04.007

14. W. Xu, H. Shu, L. Wang, G. Fan, Bifurcation-induced species coexistence in a stage-structured intraguild predation model, *SIAM J. Appl. Math.*, **85** (2025), 662–686. https://doi.org/10.1137/24M1640392

15. R. S. Cantrell, C. Cosner, *Spatial ecology via reaction–Diffusion equations*, John Wiley & Sons, 2004. https://doi.org/10.1002/0470871296

16. J. R. Potts, M. A. Lewis, Spatial memory and taxis-driven pattern formation in model ecosystems, *Bull. Math. Biol.*, **81** (2019), 2725–2747. https://doi.org/10.1007/s11538-019-00626-9

17. B. Zhang, K. Y. Lam, W. M. Ni, R. Signorelli, K. M. Collins, Z. Fu, et al., Directed movement changes coexistence outcomes in heterogeneous environments, *Ecol. Lett.*, **25** (2022), 366–377. https://doi.org/10.1111/ele.13925

18. Y. Lou, On the effects of migration and spatial heterogeneity on single and multiple species, *J. Differ. Equ.*, **223** (2006), 400–426. https://doi.org/10.1016/j.jde.2005.05.010

19. G. Q. Sun, J. Zhang, L. P. Song, Z. Jin, B. L. Li, Pattern formation of a spatial predator–prey system, *Appl. Math. Comput.*, **218** (2012), 11151–11162. https://doi.org/10.1016/j.amc.2012.04.071

20. W. Xu, H. Shu, Z. Tang, H. Wang, Complex dynamics in a general diffusive predator–prey model with predator maturation delay, *J. Dyn. Diff. Equat.*, **36** (2024), 1879–1904. https://doi.org/10.1007/s10884-022-10176-9

21. D. Ryan, R. S. Cantrell, Avoidance behavior in intraguild predation communities: a cross-diffusion model, *Discrete Contin. Dyn. Syst.*, **35** (2015), 1641–1663. https://doi.org/10.3934/dcds.2015.35.1641

22. F. Farivar, G. Gambino, V. Giunta, M. C. Lombardo, M. Sammartino, Intraguild predation communities with anti–predator behavior, *SIAM J. Appl. Dyn. Syst.*, **24** (2025), 1110–1149. https://doi.org/10.1137/24M1632747

23. B. Abrahms, E. L. Hazen, E. O. Aikens, M. S. Savoca, J. A. Goldbogen, S. J. Bograd, et al., Memory and resource tracking drive blue whale migrations, *Proc. Natl. Acad. Sci. USA*, **116** (2019), 5582–5587. https://doi.org/10.1073/pnas.1819031116

24. H. Wang, Y. Salmaniw, Open problems in PDE models for knowledge-based animal movement via nonlocal perception and cognitive mapping, *J. Math. Biol.*, **86** (2023), 71. https://doi.org/10.1007/s00285-023-01905-9

25. S. Li, Q. Wei, X. Song, L. Dai, C. Huang, Double Hopf bifurcation generated by dual memory delays in a diffusive two-species model, *J. Appl. Math. Comput.*, **72** (2026), 101. https://doi.org/10.1007/s12190-025-02754-z

26. J. A. Merkle, H. Sawyer, K. L. Monteith, S. P. Dwinnell, G. L. Fralick, M. J. Kauffman, Spatial memory shapes migration and its benefits: evidence from a large herbivore, *Ecol. Lett.*, **22** (2019), 1797–1805. https://doi.org/10.1111/ele.13362

27. J. Shi, C. Wang, H. Wang, Diffusive spatial movement with memory and maturation delays, *Nonlinearity*, **32** (2019), 3188. https://doi.org/10.1088/1361-6544/ab1f2f

28. C. Wang, S. Yuan, H. Wang, Spatiotemporal patterns of a diffusive prey-predator model with spatial memory and pregnancy period in an intimidatory environment, *J. Math. Biol.*, **84** (2022), 12. https://doi.org/10.1007/s00285-022-01716-4

29. M. Banerjee, S. Petrovskii, Self-organised spatial patterns and chaos in a ratio-dependent predator–prey system, *Theor. Ecol.*, **4** (2011), 37–53. https://doi.org/10.1007/s12080-010-0073-1

30. J. Xu, T. Zou, Dynamics of a predator-prey model with the Allee effect for the predator induced by weighted harvesting strategy, *AIMS Math.*, **11** (2026), 578–593. https://doi.org/10.3934/math.2026025

31. Y. Song, Y. Peng, T. Zhang, Dynamics of a predator-prey model with the Allee effect for the predator induced by weighted harvesting strategy, *J. Differ. Equ.*, **300** (2021), 597–624. https://doi.org/10.1016/j.jde.2021.08.010

32. M. Liu, H. Wang, W. Jiang, Double-Hopf bifurcation and bistable asynchronous periodic orbits for the memory-based diffusion system, *SIAM J. Appl. Dyn. Syst.*, **23** (2024), 2732–2768. https://doi.org/10.1137/23M1627493

33. Q. An, E. Beretta, Y. Kuang, C. Wang, H. Wang, Geometric stability switch criteria in delay differential equations with two delays and delay dependent parameters, *J. Differ. Equ.*, **266** (2019), 7073–7100. https://doi.org/10.1016/j.jde.2018.11.025

34. Y. Ding, P. Yu, Dynamics of a pine wilt disease control model with nonlocal competition and memory diffusion, *Math. Biosci.*, **389** (2025), 109524. https://doi.org/10.1016/j.mbs.2025.109524

35. J. Shi, C. Wang, H. Wang, Spatial movement with diffusion and memory-based self-diffusion and cross-diffusion, *J. Differ. Equ.*, **305** (2021), 242–269. https://doi.org/10.1016/j.jde.2021.10.021

36. T. Zheng, L. Zhang, Y. Luo, X. Zhou, H. L. Li, Z. Teng, Stability and Hopf bifurcation of a stage-structured cannibalism model with two delays, *Int. J. Bifurcat. Chaos*, **31** (2021), 2150242. https://doi.org/10.1142/S0218127421502424

37. T. Faria, Normal forms and Hopf bifurcation for partial differential equations with delays, *Trans. Amer. Math. Soc.*, **352** (2000), 2217–2238. https://doi.org/10.1090/S0002-9947-00-02280-7

38. S. Li, S. Yuan, Z. Jin, H. Wang, Double Hopf bifurcation induced by spatial memory in a diffusive predator–prey model with Allee effect and maturation delay of predator, *Commun. Nonlinear Sci. Numer. Simul.*, **132** (2024), 107936. https://doi.org/10.1016/j.cnsns.2024.107936

39. Y. Lv, Global boundedness and spatially inhomogeneous Hopf bifurcation in a delayed predator–prey model with dual taxis, *Chaos Soliton. Fract.*, **201** (2025), 117369. https://doi.org/10.1016/j.chaos.2025.117369

40. X. Chen, M. Gao, Y. Jiang, D. Jiang, Dynamic properties of a prey–predator food chain chemostat model with Ornstein–Uhlenbeck process, *Math. Methods Appl. Sci.*, **48** (2025), 9253–9271. https://doi.org/10.1002/mma.10797

41. M. Gao, D. Jiang, J. Ding, Analysis of a chemostat model with species death rate and Ornstein–Uhlenbeck process, *J. Math. Phys.*, **66** (2025), 062702. https://doi.org/10.1063/5.0214134

42. M. Gao, X. Chen, D. Jiang, Exploring the impact of distributed delay and environmental fluctuation on food chain stability in a chemostat model, *Qual. Theory Dyn. Syst.*, **24** (2025), 149. https://doi.org/10.1007/s12346-025-01303-0

AIMS Press